

# QCD AT HIGH ENERGIES\*

**Stefano Catani**

I.N.F.N., Sezione di Firenze and Dipartimento di Fisica, Università di Firenze  
Largo E. Fermi 2, I-50125 Florence, Italy  
and  
Theory Division, CERN  
CH-1211 Geneva 23, Switzerland

## Abstract

The following topics in perturbative QCD are reviewed: recent theoretical progress in higher-order calculations; soft-gluon resummation for hard-scattering processes at large  $E_T$  and high  $x$ ; low- $x$  behaviour of structure functions and recent theoretical results on BFKL dynamics; infrared renormalons and power corrections to perturbative predictions; updated summary of  $\alpha_S$  measurements.

CERN-TH/97-371  
December 1997

---

\*Invited talk given at the XVIII International Symposium on Lepton Photon Interactions, LP97, Hamburg, Germany, July 28th–August 1st, 1997. To be published in the Proceedings.

# QCD AT HIGH ENERGIES

STEFANO CATANI

*INFN, Sezione di Firenze and Dipartimento di Fisica, Università di Firenze,  
Largo E. Fermi 2, I-50125 Florence, Italy*

*and*

*TH Division, CERN, CH-1211 Geneva 23, Switzerland*

*E-mail: catani@vxcern.cern.ch*

The following topics in perturbative QCD are reviewed: recent theoretical progress in higher-order calculations; soft-gluon resummation for hard-scattering processes at large  $E_T$  and high  $x$ ; low- $x$  behaviour of structure functions and recent theoretical results on BFKL dynamics; infrared renormalons and power corrections to perturbative predictions; updated summary of  $\alpha_S$  measurements.

## 1 Introduction

Quantum Chromodynamics (QCD) is nowadays settled as the theory of strong interactions within the Standard Model (SM) of the elementary particles. To a large extent, this achievement is the result of the theoretical and experimental progress in hadronic physics at high energies. In this kinematic regime, QCD is synonymous of ‘perturbative QCD’. This talk will cover a selection of topics, rather than results, in perturbative QCD. More comprehensive reviews of recent results on jet physics<sup>1</sup>, unpolarized<sup>2</sup> and polarized<sup>3</sup> nucleon structure functions, photon structure<sup>4</sup>, diffractive processes<sup>5</sup> and heavy-quark<sup>6</sup> production and decay are presented in other contributions to this Symposium.

Calculations at the lowest order (LO) in QCD perturbation theory give only the order of magnitude of hard-scattering cross-sections. The theoretical accuracy of perturbative-QCD predictions is instead controlled by the size of the next-to-leading order (NLO) and, in general, higher-order contributions. Section 2 is devoted to a review of the theoretical progress in perturbative calculations and also includes the results of recent measurements of  $\alpha_S$ .

Soft-gluon radiation is a source of large higher-order corrections for hard-scattering processes near the exclusive boundary of the phase space. In these cases, summation of the corrections to all orders can be important to improve the accuracy of the perturbative approach. In Sect. 3, some predictions based on soft-gluon resummation are briefly reviewed and their impact on the analysis of experimental data from high-energy colliders is discussed.

Low- $x$  physics is a topic at the border of hard and soft hadronic interactions. Section 4 summarizes present analyses of the low- $x$  behaviour of the nucleon structure function and outlines recent theoretical developments in the BFKL formulation of small- $x$  dynamics.

At high energies, non-perturbative phenomena affect perturbative predictions by contributions that are suppressed by inverse powers of the energy. Some recent theoretical ideas and phenomenological studies to quantify power corrections are discussed in Sect. 5.

A world summary of  $\alpha_S$  determinations is presented in Sect. 6 and some concluding remarks are left to Sect. 7.

## 2 Higher-order calculations in perturbation theory

The evaluation of perturbative corrections to hard-scattering cross-sections requires the computation of higher-order Feynman diagrams that involve real and virtual partons. In this computation one has to deal with different kinds of singularities. The customary ultraviolet singularities, present in the virtual contributions, are removed by renormalization. By adding real and virtual terms, the infrared divergences cancel in inclusive cross sections, while the left-over collinear singularities are factorized in the process-independent parton distributions and fragmentation functions.

Because of this complicated pattern of singularities, it is natural to divide QCD observables into two different classes, according to their degree of inclusiveness.

### 2.1 Completely inclusive quantities: NNLO predictions and recent $\alpha_S$ determinations

Fully inclusive quantities are infrared- and collinear-safe observables that depend on a single momentum scale. They can be expressed as a simple power series expansion in  $\alpha_S$ .

The best known observables of this type are the total hadronic cross-section in  $e^+e^-$  annihilation and the hadronic branching ratio of the  $Z^0$ . In Ref. <sup>7</sup>, these observables were computed up to next-to-next-to-leading order (NNLO) in perturbation theory, i.e. to relative accuracy  $\mathcal{O}(\alpha_S^3)$  with respect to the lowest-order approximation. These calculations have recently been confirmed by an independent re-evaluation <sup>8</sup>. Using these results, one can parametrize <sup>9</sup> the hadronic branching ratio of the  $Z^0$  as follows

$$R_Z = \frac{\Gamma_{\text{had}}(M_Z)}{\Gamma_{\text{lep}}(M_Z)} \simeq R_0 \left[ 1 + 1.06 \frac{\alpha_S}{\pi} + 0.9 \left( \frac{\alpha_S}{\pi} \right)^2 - 15 \left( \frac{\alpha_S}{\pi} \right)^3 \right] + \mathcal{O} \left( \left( \frac{1}{M_Z} \right)^p \right), \quad (1)$$

where the factor  $R_0$  includes the electroweak radiative corrections and, in particular, depends on the values of the masses of the top quark and Higgs boson. The term  $\mathcal{O}((1/M_Z)^p)$  stands for non-perturbative power corrections (cf. Sect. 5).

Other quantities, which have been computed at NNLO, are the hadronic width of the  $\tau$  lepton <sup>10,11</sup> and the deep inelastic scattering (DIS) sum rules <sup>12</sup>, namely the Gross-Llewellyn Smith sum rule <sup>13</sup> and the polarized <sup>14</sup> and unpolarized Bjorken sum rules.

Fully inclusive observables are the simplest quantities that can accurately be evaluated in QCD perturbation theory. Their (relative) simplicity from the computational viewpoint follows from kinematics. Since these observables are completely inclusive, no phase-space restriction has to be applied. Real and virtual contributions can be combined at the integrand level and this produces the cancellation of infrared and collinear singularities before performing the relevant phase-space integrations. Owing to these features, general techniques have been available for some time <sup>15</sup> to carry out NNLO calculations in analytic form. These techniques are suitable for automatic implementations in computer codes <sup>16</sup>.

The high accuracy of the theoretical predictions for these observables derives from the availability of NNLO calculations and from the fact that non-perturbative power corrections can be controlled by operator product expansions <sup>17</sup> (OPEs) and are relatively small (in general,  $p \geq 2$  and, in particular,  $p = 4$  in Eq. (1)). Because of these reasons, fully inclusive observables are particularly suitable for  $\alpha_S$  determination.

The cleanest and, in principle, most accurate determination of  $\alpha_S$  is that performed at the  $Z^0$  peak. Here, effects of power corrections are strongly suppressed because of the large value of the  $Z$  mass, and the theoretical uncertainty due to perturbative-QCD contributions beyond NNLO is estimated to be  $(\Delta\alpha_S)_{QCD} = \pm 0.002$ . In practice, however, the value of  $\alpha_S$  obtained in this way is quite sensitive to the assumption that electroweak interactions are accurately described by the SM. For instance, extracting  $\alpha_S(M_Z)$  from Eq. (1), one has<sup>18</sup>

$$\alpha_S = (\alpha_S)_{S.M.} - 3.2 \frac{\delta\Gamma_{\text{had}}}{(\Gamma_{\text{had}})_{S.M.}} . \quad (2)$$

One can see that a variation of the hadronic width by one per mille with respect to the value expected from the SM produces an effect on  $\alpha_S$  that is larger than the QCD uncertainty.

Using a fixed top mass,  $m_t = 175.6 \pm 5.5 \text{ GeV}$ , and the experimental value of  $R_Z$  reported at the 1997 summer conferences<sup>19</sup>, one obtains from Eq. (1)

$$\alpha_S(M_Z) = 0.124 \pm 0.004 (\text{exp.}) \pm 0.002 (m_H) , \quad (3)$$

where the central value corresponds to the Higgs mass  $m_H = 300 \text{ GeV}$  and the second error is due to the variation of  $m_H$  in the range  $60 \text{ GeV} < m_H < 1 \text{ TeV}$ . The sensitivity of  $\alpha_S$  to the SM assumption can be reduced by considering a global fit to electroweak data. In this case  $\alpha_S$  mainly depends on  $R_Z$ , the total width  $\Gamma_Z$  and the peak value of the hadronic cross section  $\sigma_h^0$ . The simultaneous fit of  $m_t, \alpha_S, m_H$  gives<sup>19</sup>  $m_t = 173.1 \pm 5.4 \text{ GeV}$  and

$$\alpha_S(M_Z) = 0.120 \pm 0.003 (\text{exp.}) , \quad m_H = 115_{-66}^{+116} \text{ GeV} . \quad (4)$$

The difference between the values (3) and (4) for  $\alpha_S$  comes from a shift ( $\sim -0.002$ ) produced by the new entry  $\Gamma_Z$  and a further shift ( $\sim -0.002$ ) due to the different central value of  $m_H$ . This shows that, within a global SM fit,  $\alpha_S$  is still quite sensitive to  $m_H$ . This dependence can be parametrized as follows<sup>18</sup>

$$(\Delta\alpha_S)_{m_H} = 0.0023 x_H (1 + 0.2 x_H) , \quad x_H \equiv \ln(m_H/100 \text{ GeV}) . \quad (5)$$

Much theoretical work<sup>20</sup> has recently been devoted to the calculation of quark-mass corrections to current-current correlators. These corrections are important for measurements of  $\alpha_S$  from low-energy  $e^+e^-$  data.

These results and estimates of non-perturbative contributions (along the lines of similar analyses for the hadronic decay of the  $\tau$  lepton<sup>10</sup>) have been used<sup>21</sup> to determine  $\alpha_S$  from the  $e^+e^-$  hadronic cross-section at the  $\Upsilon$  resonance. This NLO determination gives

$$\alpha_S(4.1 \text{ GeV}) = 0.228_{-0.030}^{+0.045} , \quad (6)$$

where the error is dominated by the theoretical uncertainty. The corresponding value evolved to the  $Z^0$  mass is  $\alpha_S(M_Z) = 0.119_{-0.008}^{+0.010}$  and has to be compared with a previous determination<sup>22</sup>,  $\alpha_S(M_Z) = 0.109 \pm 0.001$ , based on LO predictions.

Measurements of  $\alpha_S$  from the continuum in  $e^+e^-$  annihilation at low energies have typically large experimental errors due to poor statistics. The new measurement submitted by the CLEO Collaboration to this Symposium is<sup>23</sup>

$$\alpha_S(10.52 \text{ GeV}) = 0.20 \pm 0.01(\text{stat.}) \pm 0.06(\text{syst.}) . \quad (7)$$

Note that, because of the large amount of data collected at CESR just below the  $\Upsilon$  resonance, the statistical error is no longer dominant. The systematic error is theoretical (uncertainties in QED radiative corrections) and experimental (estimates of backgrounds and detector efficiencies).

## 2.2 Inclusive quantities: NLO calculations and general algorithms

QCD calculations beyond LO for inclusive quantities are much more involved. Owing to the complicated phase space for multiparton configurations, analytic calculations are in practice impossible for most of the distributions. Moreover, infrared and collinear singularities, separately present in the real and virtual contributions at the intermediate steps, have to be first regularized by analytic continuation in a number of space-time dimensions  $d = 4 - 2\epsilon$  different from four. This analytic continuation prevents a straightforward implementation of numerical integration techniques.

Methods to overcome these problems are known. They consist in using hybrid analytical/numerical procedures: one must somehow extract and simplify the singular parts and treat them analytically; the remainder is treated numerically, independently of the full complications of the actual calculation. These methods were first<sup>24</sup> used to evaluate 3-jet cross sections in  $e^+e^-$  annihilation and were then applied to other cross sections<sup>25</sup>, adapting the method each time to the particular process. This is very time-consuming and has required lot of effort to produce new NLO calculations.

Only recently has it become clear that these methods are generalizable in a process-independent manner. The key observation is that the singular parts of the QCD matrix elements can be singled out in a general way by using the factorization properties of soft and collinear radiation. Owing to this universality, the methods have led to general algorithms<sup>26,27,28</sup> for NLO QCD calculations.

The various algorithms use different methods and techniques (phase-space slicing<sup>26</sup>, subtraction method<sup>27</sup>, dipole formalism<sup>28</sup>) to achieve a common goal. All the analytical work that is necessary to evaluate and cancel the infrared singularities is carried out once and for all. The final output of the algorithms is given in terms of effective matrix elements that can be automatically constructed starting from the original (process-dependent) matrix elements and universal (process-independent) factors. The effective matrix elements can be integrated numerically or analytically (whenever possible) over the available phase space in four dimensions to compute the actual value of the NLO cross section. If the numerical approach is chosen, Monte Carlo integration techniques can be easily implemented to provide general-purpose Monte Carlo programs for carrying out NLO calculations in any given process.

Using these algorithms, the computation of inclusive quantities at NLO essentially amounts to the evaluation of the original matrix elements. Since efficient techniques<sup>29</sup> (based on helicity formalism and colour-subamplitude decompositions) are available for calculating real matrix elements, the computation of the matrix elements for the virtual contribution remains the only real obstacle to perform new NLO calculations.

In recent years, this obstacle was greatly reduced by the introduction of new tools<sup>30</sup>, inspired by string-theory methods, for the evaluation of one-loop amplitudes. One-loop

matrix elements involving up to five massless partons are known<sup>31</sup> and the computation of those with four massless partons and a vector boson has been completed recently<sup>32</sup>.

The relevance of the theoretical progress that I have briefly outlined is witnessed by the accelerated production rate of new NLO calculations. These include, for instance, 4-jet cross sections<sup>33</sup> and mass quark corrections<sup>34</sup> to 3-jet observables in  $e^+e^-$  annihilation. The complete calculation for 3-jet cross sections in hadron collisions<sup>35</sup> is expected to appear soon.

The theoretical accuracy of NLO predictions for inclusive observables can reach the level of 10–20%, although in some notable cases (e.g. production cross sections of charm and bottom quarks<sup>6</sup> and direct photons<sup>1</sup>) theoretical uncertainties are much larger and the agreement with data is poor. This accuracy is very important for physics studies within and beyond the SM. The comparison between NLO predictions and high-energy collider data is discussed in Ref.<sup>1</sup> and in the following sections. The new calculations mentioned above are extremely valuable for further studies such as, for instance, to obtain stronger constraints on the elusive light gluino<sup>33,36</sup> and to measure the running of the  $b$ -quark mass<sup>34,37</sup>.

The extension to higher orders of the NLO techniques described in this section is still a challenge for theorists. The high experimental accuracy of LEP and SLC data demands improved perturbative-QCD predictions and efforts in this direction.

### 3 All-order resummation, high $E_T$ , high $x$

Higher-order perturbative contributions are certainly important for studies of QCD observables close to the exclusive boundary of the phase space. Although infrared and collinear singularities cancel in inclusive cross sections upon adding real and virtual contributions, in this kinematic regime real emission is strongly inhibited. The ensuing mismatch of real and virtual corrections generates double-logarithmic terms of the type  $(\alpha_S L^2)^n$ , where  $L = \ln 1/y$ , and  $y$  generically denotes the distance from the exclusive boundary. For instance,  $y = y_{\text{cut}}$  can be the resolution parameter for the transverse size of jets in  $e^+e^-$  annihilation, or  $y = 1 - 2E_T/\sqrt{S}$ , where  $E_T$  is the transverse energy of jets produced in hadron collisions at the centre-of-mass energy  $\sqrt{S}$ , or  $y = 1 - x$ , where  $x$  is the Bjorken variable in DIS processes.

In all these processes, when  $y \ll 1$  the logarithmically-enhanced terms of infrared origin spoil the convergence of the fixed-order expansion in  $\alpha_S$ . Accurate predictions require the evaluation and (whenever feasible) the resummation of this class of contributions to all orders in perturbation theory<sup>38</sup>. In the following I briefly discuss some examples of soft-gluon resummation in lepton and hadron collisions. Transverse-momentum distributions of vector bosons and di-photon systems are reviewed elsewhere<sup>1</sup> in these proceedings.

#### 3.1 Jet rates and event shapes in $e^+e^-$ annihilation

A detailed understanding of logarithmically-enhanced terms exists for jet rates<sup>39</sup> and for many shape variables<sup>40,41</sup> in  $e^+e^-$  annihilation in the two-jet limit. In these cases all-order resummation takes an exponentiated form. For instance, using the  $k_\perp$ -algorithm<sup>39,42</sup> to

define jets, the 2-jet rate  $R_2$  is given by<sup>39,43</sup>

$$R_2(\alpha_S(Q), y_{\text{cut}}) \equiv \frac{\sigma_{2jet}}{\sigma_{tot}} = \exp \left\{ -\frac{2C_F}{\pi} \int_{Q\sqrt{y_{\text{cut}}}}^Q \frac{dk}{k} \alpha_S(k) \ln \frac{Q^2}{k^2} + \dots \right\} , \quad (8)$$

where  $y_{\text{cut}}$  is the jet resolution parameter,  $Q$  is the  $e^+e^-$  centre-of-mass energy and the dots denote subleading contributions. Note that the exponent involves a double-logarithmically-weighted integral of the QCD coupling. The effective scale  $k$  at which  $\alpha_S$  is evaluated corresponds to the transverse momentum exchanged at the elementary QCD vertices rather than to the total momentum  $Q$ . Using the QCD running,  $\alpha_S(k) = \alpha_S(Q)/(1+2\beta_0\alpha_S(Q)\ln k/Q)$ , one can nonetheless perform the integral in Eq. (8) and explicitly obtain  $R_2$  as a function of  $\alpha_S(Q)$  and  $L = \ln 1/y_{\text{cut}}$ .

In general, shape variable and jet rates can be written as follows<sup>44</sup>

$$R(\alpha_S, y) = C(\alpha_S)\Sigma(\alpha_S, L) + D(\alpha_S, y) , \quad (9)$$

$$\Sigma(\alpha_S, y) = \exp \{ Lg_1(\alpha_S L) + g_2(\alpha_S L) + \dots \} , \quad C(\alpha_S) = 1 + \sum_{n=1}^{\infty} C_n \alpha_S^n , \quad (10)$$

where  $D(\alpha_S, y)$  vanishes as  $y \rightarrow 0$  order-by-order in perturbation theory. In the expression (9) the singular  $\ln y$ -dependence is entirely included in the effective form factor  $\Sigma$ , given in Eq. (10). The function  $Lg_1$  resums all the *leading* contributions  $\alpha_S^n L^{n+1}$ , while  $g_2$  contains the *next-to-leading* logarithmic terms  $\alpha_S^n L^n$  and so forth. Equation (10) represents an improved perturbative expansion in the two-jet region  $y \ll 1$ . Once the functions  $g_i$  have been computed, one has a systematic perturbative treatment of the shape distribution throughout the region of  $y$  in which  $\alpha_S L \lesssim 1$ , which is much larger than the domain  $\alpha_S L^2 \ll 1$  in which the fixed-order expansion in  $\alpha_S$  is applicable. Furthermore, the resummed expressions (9) and (10) can consistently be matched with fixed-order calculations. In particular, one can consider the next-to-leading logarithmic approximation (NLLA) as given by the functions  $g_1$  and  $g_2$  and combine them with the complete NLO results<sup>24,45</sup> (after subtracting the resummed logarithmic terms in order to avoid double counting), to obtain a prediction ( $\mathcal{O}(\alpha_S^2)$ +NLLA) which is everywhere at least as good as the fixed-order result, and much better as  $y$  becomes small.

Detailed experimental studies<sup>46</sup> performed at LEP 1 and the SLC proved that resummed predictions substantially improve the QCD description of the data. These analyses led to determinations of  $\alpha_S$  from hadronic final states with reduced theoretical uncertainty with respect to pure NLO calculations. The combined value from SLD and the four LEP experiments is  $\alpha_S(M_Z) = 0.122 \pm 0.001(\text{exp.}) \pm 0.006(\text{th.})$ .

Resummed calculations were also compared with  $e^+e^-$  data at lower energies, namely at PEP<sup>47</sup> ( $Q = 29$  GeV) and TRISTAN<sup>48</sup> ( $Q = 58$  GeV). A re-analysis of the data recorded in 1981–1986 by the JADE detector at PETRA has been presented recently<sup>49</sup>. This analysis provides measurements of  $\alpha_S$  at three different centre-of-mass energies,  $\alpha_S(22 \text{ GeV}) = 0.161$ ,  $\alpha_S(35 \text{ GeV}) = 0.143$ ,  $\alpha_S(44 \text{ GeV}) = 0.137$ . The energy dependence of these values is in agreement with the QCD expectation and corresponds to

$$\alpha_S(M_Z) = 0.122_{-0.006}^{+0.008} , \quad (11)$$

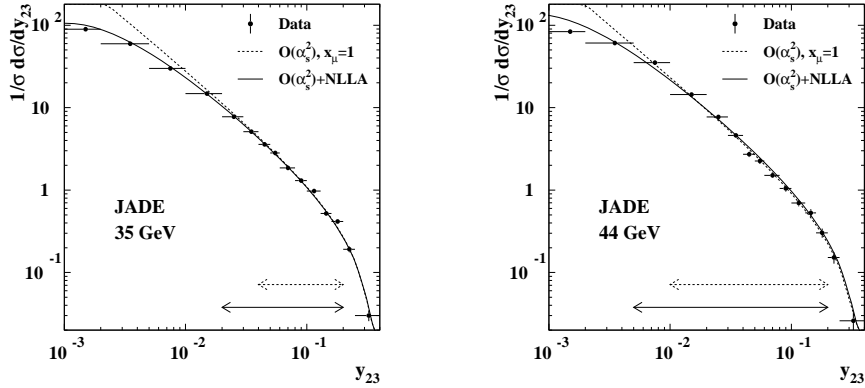


Figure 1: The differential 2-jet rates,  $dR_2/dy_{23}$  ( $y_{23} \equiv y_{\text{cut}}$ ), measured at  $Q = 44, 35$  GeV, are shown after correction to the parton level. The solid and dashed lines correspond to the results of fits with resummed and fixed-order calculations, respectively. Note the extension of the fit range (denoted by the arrow) towards the small- $y_{23}$  region in the case of resummed predictions.

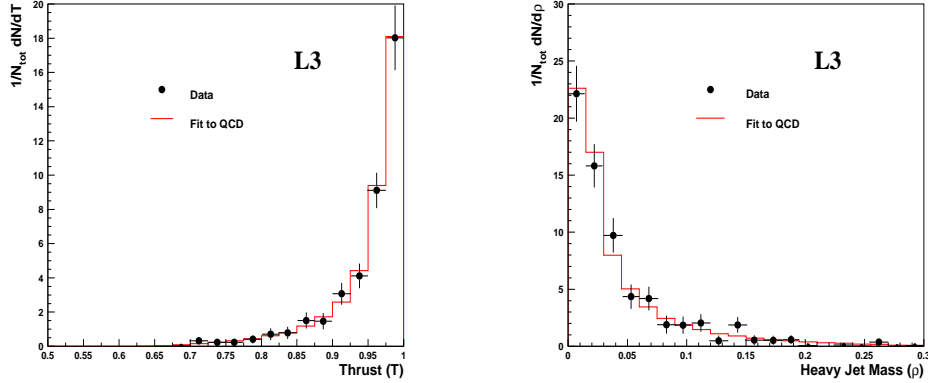


Figure 2: Measured distributions of thrust  $T$  (left) and scaled heavy jet mass  $\rho$  (right) in comparison with  $\mathcal{O}(\alpha_S^2)$ +NLLA QCD predictions at  $Q = 172$  GeV.

where the error is dominated by the theoretical uncertainty. The result (11) improves a previous determination,  $\alpha_S(M_Z) = 0.119 \pm 0.014$ , based on NLO predictions. The improvement is due to the use of more observables (see, e.g., Fig. 1) and to the inclusion of more detailed systematic studies.

The most recent data<sup>50</sup> on hadronic events from LEP 2 around  $Q = 133, 161$  and  $172$  GeV are well described by QCD predictions. Resummed calculations are quite valuable because they can be used for studies of hadronic observables close to the 2-jet region (Fig. 2), thus increasing the (otherwise very limited) statistics. The ensuing first measurements of  $\alpha_S$  at these new energies are summarized in Sect. 6. Assuming the QCD running, the combined LEP 2 average gives  $\alpha_S(M_Z) = 0.115 \pm 0.008$ .

### 3.2 Hadron collisions at high $E_T, Q^2$ and $x$

At high-energy hadron colliders, the region close to the kinematic boundary of the phase space is the most sensitive to possible signals<sup>51,52</sup> of new physics. Reliable QCD pre-



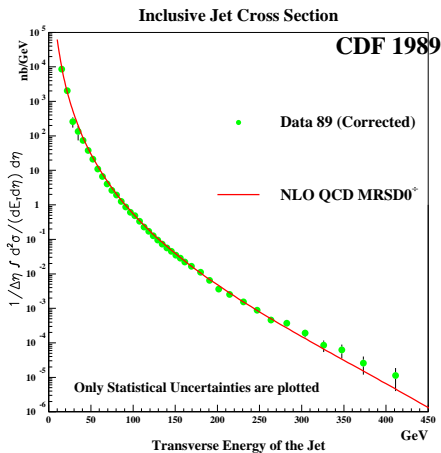


Figure 3: One-jet inclusive cross-section in  $p\bar{p}$  collisions at 1.8 TeV.

dictions are thus important not only to test the SM but also to correctly estimate SM backgrounds. Note that these predictions depend on an extra non-perturbative input with respect to  $e^+e^-$  collisions: the parton densities of the incoming hadrons to be convoluted with hard-scattering cross-sections. The present knowledge of the parton densities is reviewed elsewhere<sup>2</sup> in these proceedings.

The top quark is produced relatively close to threshold at the Tevatron<sup>53</sup>. Calculations of its production cross-section, based on NLO QCD<sup>54</sup> and including soft-gluon resummation, were performed in Refs. <sup>55–59</sup>. The results disagree on soft-gluon effects. The disagreement does not regard the general framework<sup>60,61</sup> to carry out the resummation, but the proper way to implement resummed formulae in actual computations of hadronic cross-sections.

The differences between Refs. <sup>55,56,58</sup> do not have a large impact on top-quark phenomenology: the various numerical results are consistent within uncertainty estimates and no sizeable reduction of the present experimental error is expected. However, the use of different approaches<sup>55,56,59</sup> to soft-gluon resummation in hadron collisions can be more relevant in other processes as, for instance, in the case of jet production at large transverse energy  $E_T$ .

The one-jet inclusive cross-section measured at the Tevatron<sup>1</sup> impressively agrees with NLO QCD predictions<sup>62</sup> over almost 9 orders of magnitude (Fig. 3). However, the CDF Collaboration reported<sup>51</sup> an excess of events at high  $E_T$  ( $E_T \gtrsim 250$  GeV). The present situation<sup>1,63</sup> can be summarized as follows (Fig. 4): CDF still sees an excess while D0 does not and, nonetheless, CDF and D0 data are consistent within experimental errors (Fig. 5). Previous data from the two experiments could not be compared directly as they probe different regions of jet pseudorapidity  $\eta$ . A new D0 analysis in the same pseudorapidity range as that of CDF shows (Fig. 5) that the CDF data lie above the D0 results, but within the D0 uncertainty band.

The origin of the differences between these experimental results has to be further clarified. The angular distribution for two-jet events<sup>64</sup> is in good agreement with NLO QCD

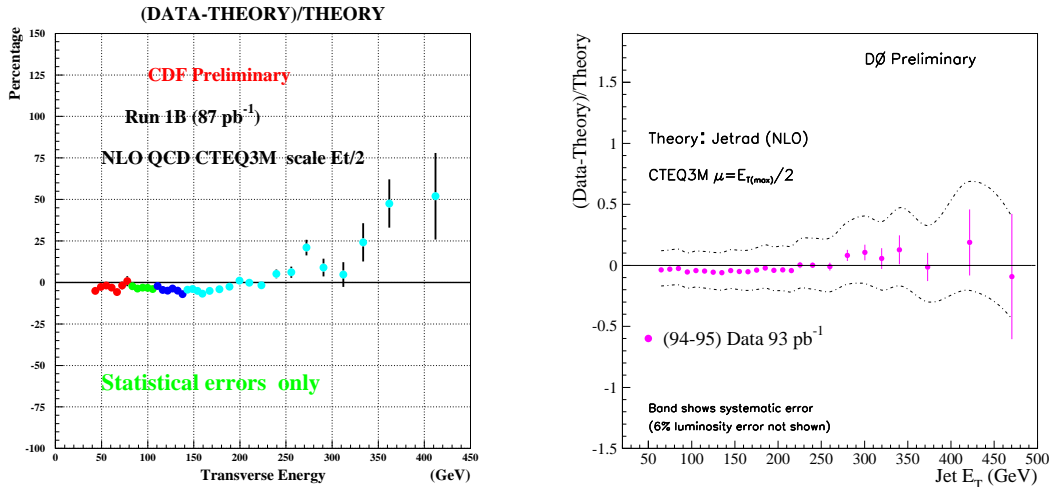


Figure 4: Relative difference between the inclusive jet cross-section and NLO predictions. CDF (left) and DØ (right) data refer to the pseudorapidity ranges  $0.1 < |\eta| < 0.7$  and  $|\eta| < 0.5$ , respectively. CDF systematic errors are not shown.

calculations, suggesting that the possible high- $E_T$  excess may have an explanation within the framework of QCD rather than originating from new physics. Independently, the accuracy of the QCD predictions has to be carefully estimated.

Using different conventional sets<sup>65,66,67</sup> of parton distributions and different values of factorization/renormalization scales, NLO predictions for the one-jet cross-section in the range  $50 \lesssim E_T \lesssim 400$  vary by approximately 15%. As for soft-gluon effects, one can at present estimate an increase of the cross section by  $\sim 20\%$ <sup>57</sup> or by less than 10%<sup>59</sup>, depending on the resummation approach used. Further investigations are warranted. The fact that the estimate in Ref.<sup>59</sup> is within the variation of the NLO predictions may suggest that higher-order QCD corrections are under control.

Note, however, that the true uncertainty due to parton densities can be larger. As shown by the CTEQ Collaboration<sup>68</sup>, including the CDF data in global fits to parton distributions, there is enough flexibility to increase the gluon density at large  $x$  and enhance by 25–30% the NLO predictions for the single-jet distribution at high  $E_T$ .

The HERA experiments have reported<sup>52</sup> an excess of DIS events at large values of  $Q^2$  ( $15\,000 \lesssim Q^2 \lesssim 50\,000 \text{ GeV}^2$ ) and  $x$  ( $0.5 \lesssim x \lesssim 0.7$ ). This has raised considerable interest in the high-energy physics community<sup>69</sup>. The measured excess has decreased as the integrated luminosity increased<sup>70</sup>, but it still deserves attention<sup>69</sup>.

The observed excess is with respect to the SM expectation based on QCD predictions. Their accuracy relies on estimates of beyond-NLO perturbative corrections and on accurate determinations of non-perturbative parton densities.

In DIS processes at large  $x$ , logarithmically-enhanced contributions due to soft-gluon emission can be sizeable. We have implemented<sup>71</sup> the corresponding resummation formulae<sup>72</sup> to estimate the order of magnitude of the effect in the relevant HERA region. The results of this exercise are illustrated in Fig. 6. The overall sign of the resummation effect

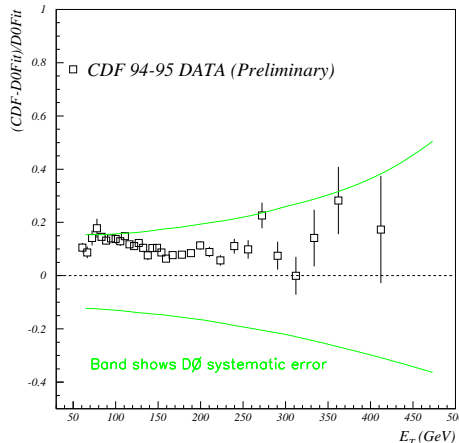


Figure 5: Relative difference between CDF data and a fit of the D0 data in the range  $0.1 < |\eta| < 0.7$ . The systematic band is mainly due to the D0 jet energy scale uncertainty.

on the measured structure functions is negative because multigluon radiation increases the scaling violation at large  $x$ . The decrease in the predictions is nonetheless extremely small for  $x \lesssim 0.7$ , so that the NLO evolution is safe in this kinematics region.

The main source of uncertainty in the SM predictions<sup>52</sup> thus comes from the extraction of the parton (quark) densities from low- $Q^2$  data. From a dedicated fit<sup>73</sup> to SLAC, BCDMS, NMC data at large  $x$ , the uncertainty is estimated to be  $\sim 10\%$ . This value is larger than the differences ( $\sim 6\%$ ) obtained by calculations that use different sets<sup>65,66,67</sup> of conventional parton densities (cf. Fig. 3 in Ref. <sup>73</sup>). Sizeable additional effects due, for instance, to a new component<sup>74</sup> in the quark densities at extremely large values of  $x$ , can be excluded<sup>69</sup> by combining HERA data in the neutral- and charged-current channels.

#### 4 Low- $x$ physics and structure functions

Strong-interaction dynamics in the small- $x$  regime<sup>75</sup> is a main challenge to QCD. Much progress in the field has been prompted by measurements of structure functions<sup>2</sup> and diffractive interactions<sup>5</sup> at HERA in a kinematic range that extends down to  $x \sim 10^{-4}$ . The present status of small- $x$  physics for hard-scattering processes involving two transverse-momentum scales (e.g. forward jet production in DIS, two-jet inclusive measurements at large rapidity gaps) is reviewed in Ref. <sup>1</sup>.

I shall consider single-scale processes and, in particular, DIS structure functions at low  $x$ . In this case, one can study<sup>2</sup> the transition between the perturbative and non-perturbative regimes, and this may eventually lead to a QCD understanding of soft hadronic physics at high energy.

##### 4.1 Confronting DGLAP with BFKL

The QCD analysis of low- $x$  structure functions has to deal with a non-trivial interplay between perturbative evolution towards the hard scale  $Q^2$  and non-perturbative behaviour

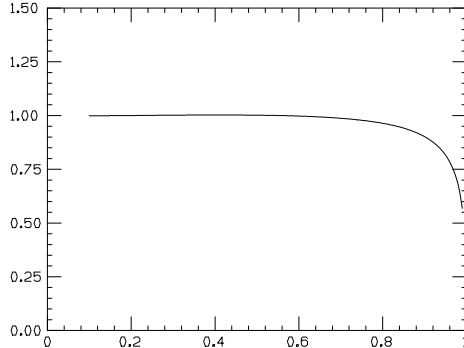


Figure 6: The ratio  $F^{\text{res}}(x, Q^2)/F^{\text{NLO}}(x, Q^2)$  at  $Q^2 = 30\,000 \text{ GeV}^2$ . The DIS structure functions  $F^{\text{NLO}}$  and  $F^{\text{res}}$  are respectively obtained by  $Q^2$ -evolution in NLO and including soft-gluon resummation. The  $Q^2$ -evolution is performed by starting from the scale  $Q_0^2 = 10 \text{ GeV}^2$  with an input structure function  $F(x, Q_0^2) \sim (1-x)^3$ .

of the parton densities. This complicates the answer to a basic question that regards the region of applicability of the QCD parton model. How far in  $x$  can we safely use the DGLAP evolution equations<sup>76</sup> before they have to be supplemented with BFKL-type<sup>77</sup> effects?

To discuss this point let me recall the main steps in the QCD analysis of the structure functions. The measurement of the proton structure function  $F_2(x, Q^2) \sim f_S(x, Q^2)$  directly determines the sea-quark density  $f_S = x(q + \bar{q})$ . Then one can use the DGLAP evolution equations (the symbol  $\otimes$  denotes the convolution integral with respect to  $x$ ),

$$dF_2(x, Q^2)/d \ln Q^2 \sim P_{qq} \otimes f_S + P_{qg} \otimes f_g \quad , \quad (12)$$

$$df_g(x, Q^2)/d \ln Q^2 \sim P_{gq} \otimes f_S + P_{gg} \otimes f_g \quad , \quad (13)$$

to extract a gluon density  $f_g(x, Q^2) = xg(x, Q^2)$  that agrees with the measured scaling violation in  $dF_2(x, Q^2)/d \ln Q^2$  (according to Eq. (12)) and fulfils the self-consistency equation (13).

The perturbative-QCD ingredients in this analysis are the Altarelli–Parisi splitting functions  $P_{ab}(\alpha_S(Q), x)$ . They are computable as power-series expansions in  $\alpha_S$  and are known up to NLO accuracy. The truncation of the splitting functions at a fixed perturbative order is equivalent to assuming that the dominant dynamical mechanism leading to scaling violations is the evolution of parton cascades with strongly-ordered transverse momenta. However, at high energy this evolution takes place over large rapidity intervals ( $\Delta y \sim \ln 1/x$ ) and diffusion in transverse momentum becomes relevant. Formally, this implies that higher-order corrections to  $P_{ab}(\alpha_S, x)$  are logarithmically enhanced:

$$P_{ab}(\alpha_S, x) \sim \frac{\alpha_S}{x} + \frac{\alpha_S}{x} (\alpha_S \ln x) + \dots + \frac{\alpha_S}{x} (\alpha_S \ln x)^n + \dots \quad . \quad (14)$$

At asymptotically small values of  $x$ , resummation of these corrections is mandatory to obtain reliable predictions.

Small- $x$  resummation is, in general, accomplished by the BFKL equation<sup>77</sup>, whose structure is completely known only to leading logarithmic (LL) accuracy. In the context of

structure-function calculations, the BFKL equation provides us with resummed expressions for the splitting functions.

In the small- $x$  region the gluon channel dominates. Considering the fixed-order expansion of the splitting function, one-gluon exchange gives  $P_{gg}(\alpha_S, x) \sim \alpha_S/x$ . Then, assuming a flat  $x$ -behaviour of  $f_g$  at low momentum scales, the evolution equation (13) produces a gluon density  $f_g \sim \exp(\sqrt{\ln 1/x})$  that steeply increases in  $1/x$  at higher momentum scales<sup>78</sup>. The steep behaviour drives strong scaling violations in  $F_2$  and leads to structure functions that strongly rise as  $x$  decreases. This prediction is usually referred to as DGLAP prediction.

The increase of the gluon density is steeper after BFKL resummation. Summing the LL terms in  $P_{gg}$ , one eventually gets the power-like behaviour  $f_g \sim x^{-\lambda_g}$ , where  $\lambda_g \simeq 2.65 \alpha_S$ .

The fixed-order approach has been extensively compared with structure function data during the last few years. The NLO approximation of the DGLAP equations describes very well<sup>65,66,67,79–81</sup> the HERA data (Fig. 7), down to low values of  $Q^2 \sim 2 \text{ GeV}^2$ . The NLO QCD fits simply require slightly steep input parton densities at these low momentum scales.

From a phenomenological viewpoint, one may conclude that there is no need for BFKL-type corrections to scaling violations in the HERA kinematic region. The main reason for this is that the LL power-like behaviour of the BFKL gluon density is valid in the asymptotic regime and the approach to asymptotia is much delayed<sup>82–85</sup> by cancellations of logarithmic corrections that occur at the first perturbative orders in the gluon splitting function  $P_{gg}$ .

Nonetheless, a better way to estimate the relevance of BFKL-type corrections is to quantify the theoretical uncertainty of the NLO predictions, for instance by comparing LO and NLO results. Doing that, one can thus argue that this uncertainty is sizeable. This feature has recently been re-emphasized in Ref.<sup>81</sup>, but it was evident since the still-successful GRV parametrization<sup>65</sup> of parton densities. Going from LO to NLO, one can obtain stable predictions for the proton structure function  $F_2$ , but one has to vary the parton densities a lot, in particular the gluon. As shown in Fig. 8, the NLO gluon density sizeably differs from its LO parametrization, not only in absolute normalization but also in  $x$ -shape. This can be understood<sup>86</sup> from the fact that the scaling violation of  $F_2$  is produced by the convolution  $P_{qg} \otimes f_g$  (see the right-hand side of Eq. (12)). The quark splitting function  $P_{qg}$  behaves as

$$P_{qg}(\alpha_S, x) \simeq \alpha_S P_{qg}^{(0)}(x) \left[ 1 + 2.2 \frac{C_A \alpha_S}{\pi} \frac{1}{x} + \dots \right], \quad (15)$$

where the LO term  $P_{qg}^{(0)}(x)$  is flat at small  $x$ , whereas the NLO correction is steep. To obtain a stable evolution of  $F_2$ , the NLO steepness of  $P_{qg}$  has to be compensated by a gluon density that is less steep at NLO than at LO.

In the large- $x$  region, there is a well known correlation between  $\alpha_S$  and  $f_g$ . At small  $x$ , there is an analogous strong correlation between the  $x$ -shapes of  $P_{qg}$  and  $f_g$ . In the fixed-order DGLAP analysis of  $F_2$ , large NLO perturbative corrections at small  $x$  can be balanced by the extreme flexibility of parton density parametrizations.

This has to be kept in mind when concluding on the importance of BFKL dynamics. The NLO steepness of  $P_{qg}$  is the lowest-order manifestation of next-to-leading BFKL corrections in the quark channel. Using  $k_\perp$ -factorization<sup>87</sup> methods, these corrections were resummed to all orders<sup>88</sup> and implemented<sup>82–85,89–92</sup> in studies of structure functions. The results of

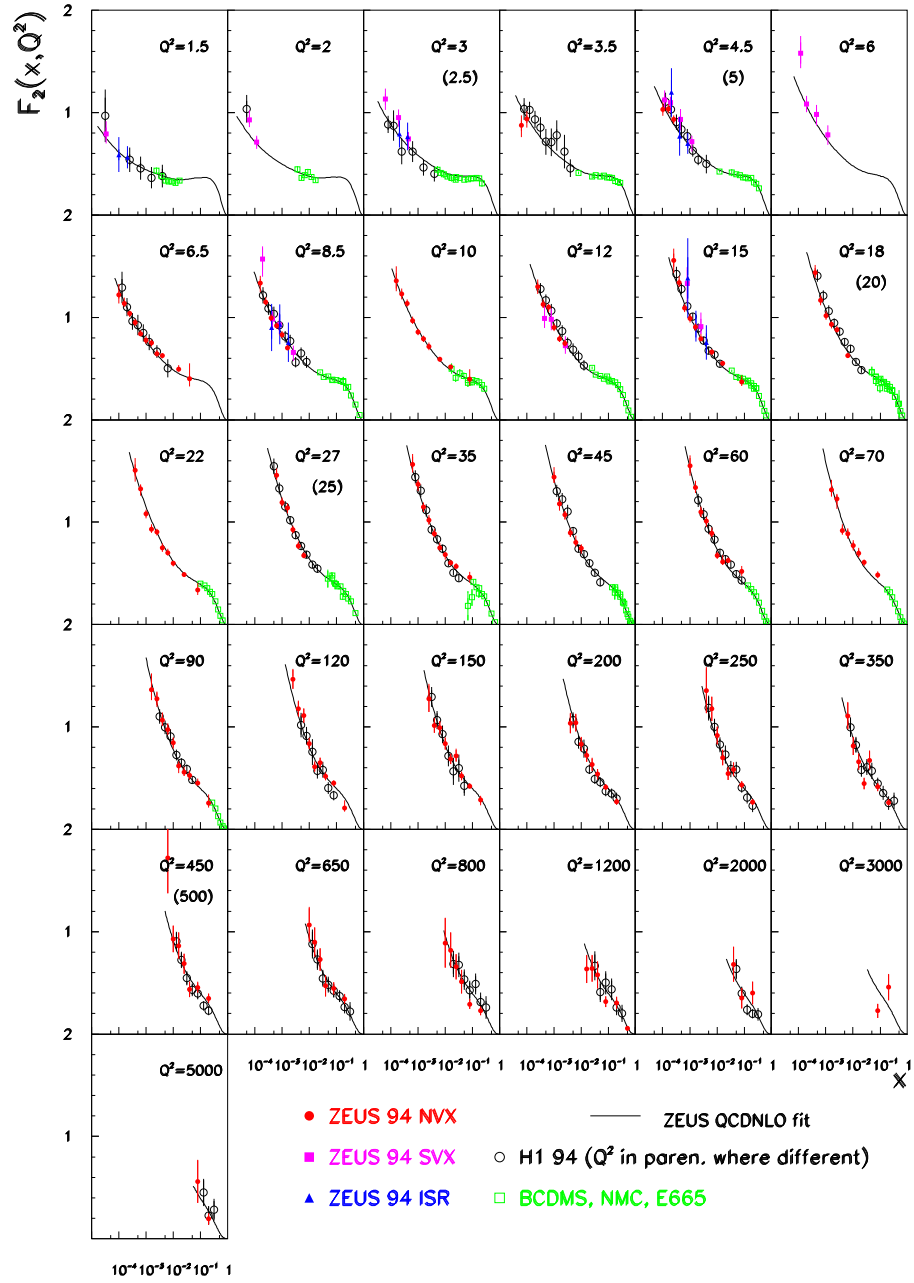


Figure 7: NLO QCD fit to low- $x$  structure function data for different values of  $Q^2$ .

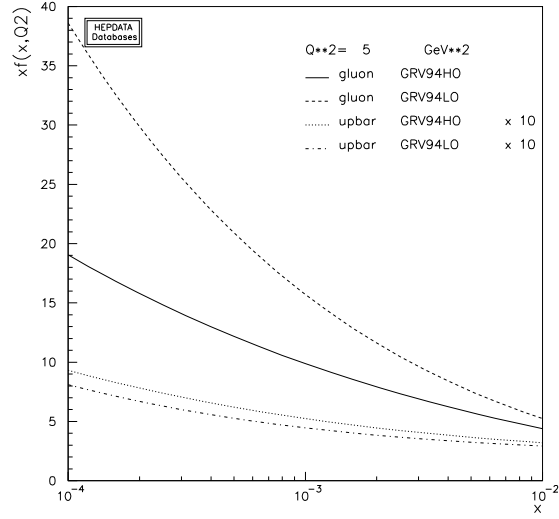


Figure 8: Comparison between the LO (GRV94LO) and NLO (GRV94HO) GRV parametrizations of the gluon and sea-quark densities at  $Q^2 = 5 \text{ GeV}^2$ .

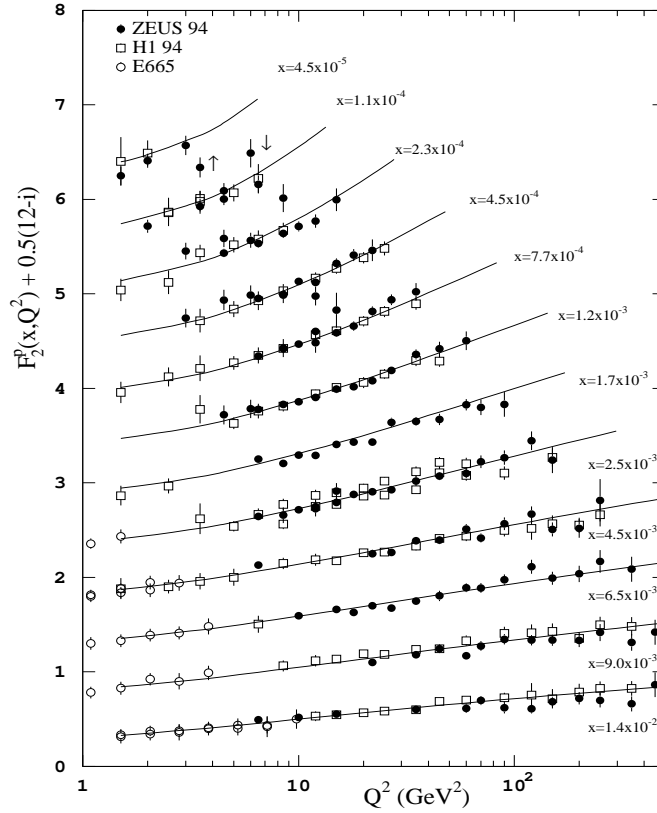


Figure 9:  $Q^2$  dependence of the proton structure function  $F_2(x, Q^2)$  at various values of  $x$ . Data from the E665, H1 and ZEUS experiments are compared with a QCD fit that includes resummation of small- $x$  contributions to LL accuracy in the gluon channel and to NLL accuracy in the quark channel.

a recent fit<sup>92</sup> are shown in Fig. 9. The present overall picture is that small- $x$  resummation leads to a description of the HERA data that is comparable to that from NLO analyses, provided that the input gluon density is less steep than the NLO  $f_g$ .

More accurate data on  $F_2$  are necessary to clarify the phenomenological relevance of BFKL effects. Measurements of other inclusive observables (for instance, the longitudinal structure function  $F_L$ <sup>93,94</sup>) can be valuable to disentangle perturbative from non-perturbative dynamics, that is, to reduce the correlation between  $P_{qg}$  and  $f_g$  in  $F_2$  analyses. At the same time, theoretical progress in higher-order calculations is very important.

#### 4.2 BFKL dynamics at NLL accuracy: recent theoretical progress

The complete evaluation of BFKL contributions to next-to-leading logarithmic (NLL) accuracy requires the computation of basic building blocks from tree-level, one-loop and two-loop amplitudes at high energy. This difficult calculational program<sup>95–98</sup>, led by the work of Fadin and Lipatov, has been completed<sup>99</sup>.

We are now in a position to start detailed investigations on phenomenological and conceptual issues related to the resummation of high-energy logarithms.

The computation of next-to-leading corrections should permit a quantitative control of normalizations, scales and factorization-scheme<sup>86,100,101</sup> uncertainties. A preliminary evaluation of the NLL corrections to the power-like behaviour of the gluon density has been performed in Ref.<sup>98</sup>. The effective power  $\lambda_g$  of the asymptotic  $x$ -shape of  $f_g$  can be written as  $\lambda_g = 2.65 \alpha_S(Q)(1 - c \alpha_S(Q))$  and, considering the scale-invariant part of the NLL BFKL contributions, the correction to  $\lambda_g$  is negative and estimated to be quite large<sup>98</sup> ( $c \sim 3.5$ ). Negative corrections to  $\lambda_g$  are also obtained by related investigations<sup>102,103</sup> on coherence effects<sup>104</sup> and the CCFM equation<sup>104,105</sup>.

A general theoretical understanding of NLL terms can clarify to what extent the BFKL formalism can be used in a purely perturbative framework and how it can be matched to the non-perturbative infrared regime. In the context of structure-function studies, one should thus be able to precisely identify the kinematic range in  $x$  and  $Q^2$  where perturbative factorization is valid and not spoiled by  $k_\perp$ -diffusion in the low-momentum region<sup>106,107</sup>.

## 5 Power corrections

A generic infrared- and collinear-safe observable  $R$  that depends on some large momentum scale  $Q$  has the following expression

$$R(Q) = R_{\text{pert}}(\alpha_S(Q)) + R_{\text{non-pert}}(Q) \quad . \quad (16)$$

The term  $R_{\text{pert}}$  denotes the perturbative component that can be calculated as power-series expansion in  $\alpha_S(Q)$  and, thus, behaves as  $(1/\ln Q)^n$ . The remaining contribution  $R_{\text{non-pert}}$  is due to non-perturbative phenomena (hadronization, multiparton scattering, ...) and is power-behaved, i.e. proportional to  $(1/Q)^p$ . Since the power  $p$  is positive,  $R_{\text{non-pert}}$  is suppressed when  $Q \rightarrow \infty$  but it can be quantitatively relevant at finite values of  $Q$ .



We have precise theoretical information on  $R_{\text{non-pert}}$  only for the processes in which OPEs are valid<sup>17</sup>. In these cases, one can write<sup>108</sup>

$$R_{\text{non-pert}}(Q) \sim \sum_{p \geq 2} C_p \left(\frac{1}{Q}\right)^p \langle O_p \rangle, \quad (17)$$

where  $\langle O_p \rangle$  denotes the vacuum expectation value of some local operator  $O_p$ , obtained by the basic quark and gluon fields. Note that in Eq. (17) we have  $p \geq 2$ , because in the theory there is no (quasi-)local operator with dimension smaller than 2. Note also that OPEs apply to few quantities such as the total cross section in  $e^+e^-$  annihilation ( $p \geq 4$ ) and the DIS structure functions ( $p \geq 2$ ). For all the other quantities, power-correction contributions are usually estimated by using phenomenological approaches (e.g. hadronization models of Monte Carlo event generators in  $e^+e^-$  annihilation).

It is evident that we need a better general understanding of power-suppressed contributions. On theoretical grounds, one would like to justify power corrections with  $p < 2$ , which are experimentally observed in  $e^+e^-$  data on event shapes (see Fig. 10), and possibly evaluate their size.

A handle on  $R_{\text{non-pert}}$  can be provided by the study of  $R_{\text{pert}}$ . It is known that the  $\alpha_S$ -series for the perturbative component  $R_{\text{pert}}$  is not a convergent series but rather an asymptotic expansion<sup>108</sup>. This implies that it is not defined in an unambiguous way. Since  $R$  is a physical observable, any ambiguity in  $R_{\text{pert}}$  has to be cancelled by a corresponding ambiguity in  $R_{\text{non-pert}}$ . Examining the series for  $R_{\text{pert}}$  at large perturbative orders, one can thus extract some information on  $R_{\text{non-pert}}$ .

Two known sources of non-convergent behaviour of the perturbative expansion are instantons and (infrared) renormalons. Roughly speaking, ‘instantons’ are related to large perturbative coefficients due to the large number of Feynman diagrams at high orders. They lead to non-perturbative corrections that are strongly power-suppressed, i.e. that have high values of  $p$ . Infrared renormalons are related to the low-momentum behaviour of the running coupling  $\alpha_S$  in Feynman diagrams.

### 5.1 Infrared renormalons

Much theoretical activity has recently been devoted to studying infrared renormalons<sup>109</sup>. A comprehensive review of the field is not feasible because even a simple list of the relevant references cannot fit into several pages of these proceedings. I shall limit myself to recalling few general points and phenomenological results.

The basic idea of the renormalon approach to power corrections is the following. The evaluation of the lowest-order perturbative contribution to  $R(Q)$  amounts to integrating tree-level Feynman diagrams over the momentum  $k$  exchanged at the elementary QCD vertices (see the left-hand side of Eq. (18)). Higher-order contributions to  $R(Q)$  are given by more complicated Feynman diagrams, including those that produce the running of the coupling constant  $\alpha_S$ . Therefore, one can approximate the effects of higher orders by the replacement  $\alpha_S \rightarrow \alpha_S(k)$  in the lowest-order term, as in Eq. (18):

$$R_{\text{pert}}(\alpha_S(Q)) \sim \alpha_S \int_0^Q \frac{dk}{Q} \left(\frac{k}{Q}\right)^p + \dots \xrightarrow{\text{higher orders}} \int_0^Q \frac{dk}{Q} \left(\frac{k}{Q}\right)^p \alpha_S(k). \quad (18)$$

The perturbative series  $R_{\text{pert}}(\alpha_S) = \sum_n R_n \alpha_S^n$  is then obtained by inserting the QCD expression for running coupling,

$$\alpha_S(k) \sim \alpha_S(Q) / [1 + 2\beta_0 \alpha_S(Q) \ln k/Q] = \sum_{n=1}^{\infty} \alpha_S^n(Q) (-2\beta_0 \ln k/Q)^{n-1} \quad , \quad (19)$$

into the right-hand side of Eq. (18) and by integrating term by term. This leads to perturbative coefficients that grow factorially at high orders:

$$R_{n+1} = n! (1/p) (2\beta_0/p)^n \quad . \quad (20)$$

The factorial growth implies that the series for  $R_{\text{pert}}(\alpha_S)$  is not convergent but can be interpreted as an asymptotic expansion. One should truncate the series at the order  $n = n_{\text{max}}$  at which the ratio of two successive terms become of order unity and estimate the truncation ambiguity  $\delta R_{\text{pert}}$  by the size of the last term that is neglected. The evaluation of  $n_{\text{max}}$  from Eq. (20) gives

$$(R_{n+1} \alpha_S^{n+1}(Q)) / (R_n \alpha_S^n(Q)) \sim 1 \quad \implies \quad n_{\text{max}} \sim p / (2\beta_0 \alpha_S(Q)) \quad . \quad (21)$$

Using this value of  $n_{\text{max}}$  and the QCD expression  $\alpha_S(Q) \sim 1/(2\beta_0 \ln Q/\Lambda_{QCD})$ , one eventually obtains an ambiguity of the perturbative component that has a power-like behaviour with respect to the large scale  $Q$ :

$$\delta R_{\text{pert}} \sim \left( R_{n+1} \alpha_S^{n+1}(Q) \right)_{n=n_{\text{max}}} \sim e^{-n_{\text{max}}} \sim \left( \Lambda_{QCD}/Q \right)^p \quad . \quad (22)$$

The recipe  $\alpha_S \rightarrow \alpha_S(k)$  of Eq. (18) to estimate the large-order behaviour of the perturbative series can be justified by summing Feynman graphs in the limit of a large number  $N_f$  of flavours<sup>110</sup> ( $N_f \rightarrow \infty$ ). Further justifications<sup>111,112</sup> follow from the structure of soft-gluon resummation formulae (cf. Eq. (8)).

Two main features of the renormalon approach to power corrections are its predictivity and its non-universality. The power  $p$  in Eq. (22) is exactly equal to that on the right-hand side of Eq. (18). Therefore, the approach unambiguously predicts the type of power correction by relating it to the dominant low-momentum behaviour of the lowest-order Feynman diagrams for any given observable. Nonetheless, the actual size of the power correction is not computable unambiguously: the ‘true’ coefficient in front of the factor  $1/Q^p$  is not related in a straightforward and universal way to that obtained by evaluating the sole lowest-order Feynman diagrams<sup>113</sup>.

## 5.2 Hadronic event shapes in $e^+e^-$ and DIS

The renormalon predictions on the power behaviour of non-perturbative corrections are in agreement<sup>114</sup> with those from OPEs when the latter apply, but can be extended also to other quantities.

Among these quantities, hadronic event shapes in  $e^+e^-$  annihilation are particularly relevant because their measured mean values receive significant non-perturbative contributions of the form  $1/Q$ . As shown in Fig. 10, parton level predictions of Monte Carlo event

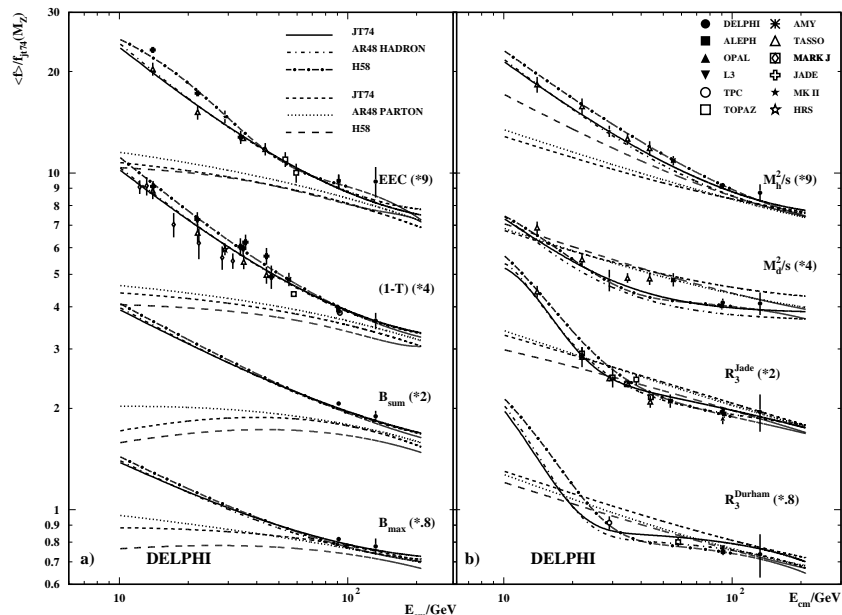


Figure 10: Energy dependence of the mean value of  $e^+e^-$  event shapes. The upper (lower) curves are the predictions of Monte Carlo event generators at hadron (parton) level.

generators fail to describe the data, but a good agreement is obtained by taking into account  $1/Q$  effects produced by the hadronization models that are built into the Monte Carlo programs. The phenomenological success of these hadronization models is well known<sup>115</sup>, but their relation with QCD dynamics is still poorly understood on a theoretical basis.

An important result of the renormalon approach is that it theoretically predicts<sup>116</sup> the existence of  $1/Q$  non-perturbative corrections to the mean values of event shapes. As for the actual size of these corrections, an attempt to overcome non-universality in renormalon calculations was proposed by Dokshitzer and Webber<sup>117,114</sup> (DW). The factorial growth of the perturbative coefficients in Eq. (20) is produced by the  $k$ -integration (see Eq. (18)) of the perturbative coupling  $\alpha_S(k)$  down to the Landau pole at  $k = \Lambda_{QCD}$ . The DW model assumes that a meaningful non-perturbative definition of  $\alpha_S(k)$  can be introduced for all values of  $k$ . Thus the integral

$$\int_0^{\mu_I} \frac{dk}{\mu_I} \alpha_S(k) \equiv \bar{\alpha}_0(\mu_I) \quad (23)$$

exists for all  $\mu_I \geq 0$  and, using Eq. (18) with  $p = 1$ , the mean value  $\langle R(Q) \rangle$  of any event shape can be written as follows

$$\langle R(Q) \rangle = \langle R_{\text{pert}}(\alpha_S(Q)) \rangle_{NLO} + \langle R_{\text{non-pert}}(Q) \rangle, \quad (24)$$

$$\langle R_{\text{non-pert}}(Q) \rangle = a_R \bar{\alpha}_0(\mu_I) (\mu_I/Q) - a_R [\bar{\alpha}_0(\mu_I)]_{NLO} (\mu_I/Q) + \dots \quad (25)$$

The first term on the right-hand side of Eq. (24) is the customary perturbative contribution evaluated up to NLO<sup>24,45</sup>, while the power correction  $\langle R_{\text{non-pert}}(Q) \rangle$  is expressed in terms of

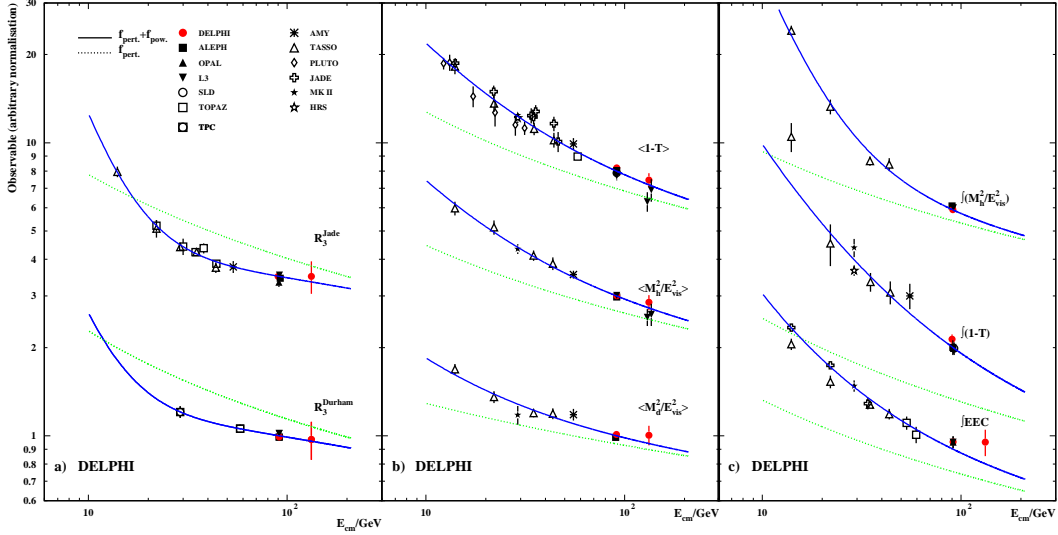


Figure 11: QCD fits for the mean value of  $e^+e^-$  event shapes. The solid lines correspond to NLO calculations combined with power corrections.

the effective non-perturbative parameter  $\bar{\alpha}_0(\mu_I)$ . To avoid double-counting of perturbative contributions, one has to consider the NLO expansion  $[\bar{\alpha}_0(\mu_I)]_{NLO}$  of the integral (23) and then subtract the second term on the right-hand side of Eq. (25). The coefficient  $a_R$  depends on the event shape  $R$  and is obtained by a direct calculation of the corresponding LO Feynman diagrams.

The DW model does not predict the absolute value of  $\langle R_{\text{non-pert}}(Q) \rangle$  for each event shape  $R$  but parametrizes all these power corrections in terms of the single ‘universal’ parameter  $\bar{\alpha}_0(\mu_I)$  and of calculable process-dependent coefficients  $a_R$ . The dots on the right-hand side of Eq. (25) stand for contributions that are more power-suppressed (i.e.  $(\mu_I/Q)^p$  with  $p > 1$ ) and for non-universality corrections to the coefficient  $a_R$  of the dominant power. These corrections come from higher-order Feynman diagrams<sup>113</sup> and, in particular, involve integrals of the type

$$\int_0^{\mu_I} \frac{dk}{\mu_I} \alpha_S^2(k) \sim \mathcal{O}(\bar{\alpha}_0^2(\mu_I)) . \quad (26)$$

If the non-perturbative parameter  $\bar{\alpha}_0(\mu_I)$  turns out to be relatively small, the corrections in Eq. (26) can be neglected in a first approximation. In phenomenological applications, the infrared matching scale  $\mu_I$  of Eq. (25) has to be chosen in the range  $Q \gg \mu_I \gg \Lambda_{QCD}$ :  $Q \gg \mu_I$ , because power corrections of higher order have to be negligible and  $\mu_I \gg \Lambda_{QCD}$ , because  $\alpha_S(\mu_I)$  still has to be in the perturbative region.

The DELPHI Collaboration performed a detailed study<sup>118,119</sup> of the energy dependence of the mean value of  $e^+e^-$  event shapes measured in the centre-of-mass energy range  $Q = 14$ – $172$  GeV. The data are well described by NLO perturbative calculations<sup>24,45</sup> supplemented with power corrections (Fig. 11). Using the predictions of the DW model for the thrust  $T$  and the heavy jet mass  $M_h$  (Fig. 11b), a combined fit of  $\alpha_S(M_Z)$  and the non-perturbative

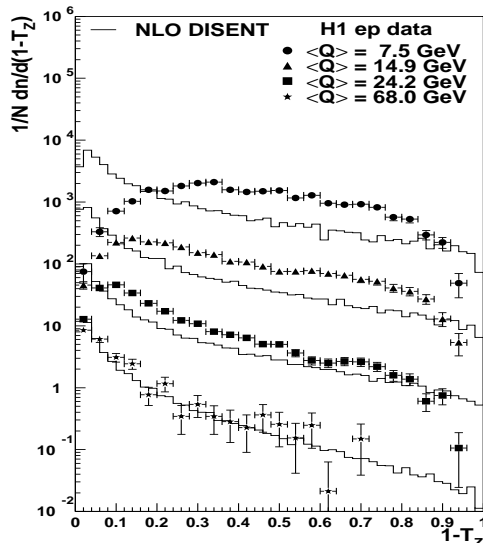


Figure 12: Distribution of the thrust ( $T_z$ ) of the current fragmentation region in DIS at different values of  $Q$ . The histograms are the corresponding NLO predictions. The spectra are multiplied by factors  $10^n$ ,  $n = 0, 1, 2, 3$  (downwards).

parameter  $\bar{\alpha}_0(\mu_I)$  gives<sup>118</sup>  $\alpha_S(M_Z) = 0.116 \pm 0.002(\text{exp.}) \pm 0.006(\text{th.})$  and

$$\bar{\alpha}_0(\mu_I = 2 \text{ GeV}) = \begin{cases} 0.534 \pm 0.012 & (\text{from } T) , \\ 0.435 \pm 0.015 & (\text{from } M_h) . \end{cases} \quad (27)$$

This determination of  $\alpha_S(M_Z)$  is consistent with those (cf. Sect. 3.1) obtained from analyses of shape distributions in which non-perturbative effects are estimated by using Monte Carlo event generators. The value of  $\bar{\alpha}_0$  in Eq. (27) suggests that corrections in the DW model can be kept under control. Similar results have been obtained by the JADE<sup>49</sup> and ALEPH<sup>120</sup> Collaborations.

Note that the fit of Fig. 11b for the jet mass difference  $M_d$  corresponds to an empirical parametrization of the power correction simply proportional to  $1/Q$  rather than to the predictions of the DW model. In fact, in this case the model gives a poor quantitative description of the data. This fact signals the presence of non-universality corrections, which are not included in the naive version of the model.

The data in Fig. 11c are obtained by averaging out the event shapes over a restricted kinematic range<sup>118</sup> that excludes the two-jet region. Note that, in the cases of  $T$  and  $M_h$ , the energy dependence of the data in Fig. 11c is stronger than that in Fig. 11b. The empirical fits of Fig. 11c are consistent with a dominant power-behaviour of the type  $1/Q^2$ . This behaviour agrees with that predicted by calculations of renormalon contributions<sup>113</sup>.

Lepton–nucleon DIS processes are an ideal place to study the  $Q$ -dependence of hadronic observables because one can vary  $Q$  over a wide range in a single experiment, thus reducing systematic uncertainties. Event shapes in DIS are analogous to those in  $e^+e^-$  annihilation, but they are usually defined in the current fragmentation region of the Breit frame. A study<sup>121</sup> of DIS event shapes in the momentum region  $Q = 7\text{--}100$  GeV has re-

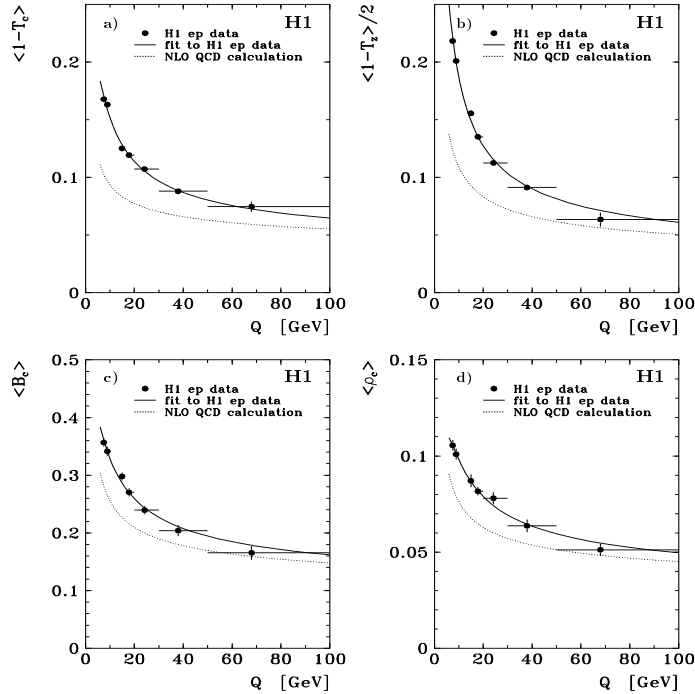


Figure 13:  $Q$ -dependence of the mean value of DIS event shapes. The solid lines are QCD fits that include NLO predictions and power corrections according to the DW model.

cently been performed by the H1 Collaboration at HERA. As shown in Fig. 12, shape distributions become narrower and jet-like when  $Q$  increases. As expected, NLO perturbative calculations<sup>122,123,124</sup> describe the data only at sufficiently large values of  $Q$ . At smaller  $Q$ , non-perturbative contributions are sizeable. The  $Q$ -dependence of the mean value of the shape variables is shown in Fig. 13, together with a combined fit that uses NLO predictions<sup>122,123,124</sup> and the DW model for power corrections<sup>125</sup>. The fit describes the data well and gives<sup>121</sup>  $\alpha_S(M_Z) = 0.118 \pm 0.001(\text{exp.})_{-0.006}^{+0.007}(\text{th.})$  and  $\bar{\alpha}_0(\mu_I = 2 \text{ GeV}) = 0.491 \pm 0.003(\text{exp.})_{-0.042}^{+0.079}(\text{th.})$ . These values are consistent with those obtained from  $e^+e^-$  event shapes.

Determinations of  $\alpha_S$  from QCD predictions that include power corrections are summarized at the end of Table 1. Besides the results from the mean values of shape variables, I have also reported a preliminary determination<sup>126</sup> from the longitudinal cross section in  $e^+e^-$  annihilation. This determination is based on the NLO calculation in Ref.<sup>127</sup> and on estimates<sup>128</sup> of power-suppressed terms.

At present, it is difficult to quantify the theoretical accuracy of these analyses. Universality of power corrections is certainly violated in its naive form<sup>129</sup>. In the DW model, the effective non-perturbative parameter is  $\bar{\alpha}_0 \sim 0.5$  and, on a phenomenological basis, one may conclude that non-universality effects are typically smaller than 50%. Future investigations on differential event shape spectra<sup>119,120,130</sup> can produce more definite quantitative results and give additional insights into the connection between hadronization and power

corrections.

## 6 Summary of $\alpha_S$

A summary of  $\alpha_S$  determinations is presented in Table 1. I shall limit myself to few comments on the comparison with last year summaries<sup>131,132</sup>.

The most relevant new result regards a redetermination<sup>133</sup> of  $\alpha_S$  from  $\nu$ -nucleon DIS. The preliminary result,  $\alpha_S(M_Z) = 0.119 \pm 0.005$ , presented by the CCFR Collaboration at the Warsaw Conference (ICHEP96), has indeed been confirmed. This result is based on a re-analysis of the CCFR data, due to a new energy calibration of the detector, and supersedes a previous and lower determination ( $\alpha_S(M_Z) = 0.111 \pm 0.006$ ). The main outcome of this is an increased average value of  $\alpha_S$  from DIS measurements. Among DIS determinations, only  $\mu$ -nucleon data from BCDMS still prefer<sup>134</sup> a value of  $\alpha_S(M_Z)$  that is (slightly) lower than those from  $e^+e^-$  annihilation.

Another new result<sup>135</sup> included in Table 1 is from scaling violation of polarized DIS structure functions. In the case of polarized DIS processes, a more accurate determination<sup>14</sup> of  $\alpha_S$  is in principle feasible from the Bjorken sum rule. At present, however, this determination suffers from uncertainties<sup>135</sup> due to the extrapolation of the data in the small- $x$  region, where polarized structure functions have not yet been measured.

The entry from  $p\bar{p} \rightarrow \text{jet} + X$  does not refer to an actual measurement, but it illustrates<sup>136</sup> the potential of jet data from hadron colliders in the determination of  $\alpha_S$ . Detailed analyses at the Tevatron experiments are in progress. The updated entry from  $\tau$  decay is from Ref.<sup>137</sup>. The theoretical uncertainty on the value<sup>138</sup> from  $J/\Psi$  and  $\Upsilon$  decays has been slightly increased according to estimates<sup>139</sup> of additional contributions from colour-octet operators.

All the other new or updated entries in Table 1 have been discussed in the previous sections. In particular, the error on  $\alpha_S$  from global fits to electroweak observables (cf. Sect. 2.1) includes the theoretical uncertainty due to the SM assumptions.

The values of  $\alpha_S$ , as a function of the energy scale  $Q$  at which they are measured, are compared with the QCD prediction of a running coupling in Fig. 14. The energy dependence of  $\alpha_S$  is distinct ( $\alpha_S(Q)$  varies by a factor of 3) and in very good agreement with the QCD running over two orders of magnitude in  $Q$ . It is thus meaningful to evolve all the results to  $\alpha_S(M_Z)$  according to perturbative QCD. A significant subset of these values is shown in Fig. 15. The subset is chosen by considering the most relevant determinations of  $\alpha_S$  from each type of process and/or energy range. Using these results, my preferred world average determination is

$$\alpha_S(M_Z) = 0.119 \pm 0.005 \quad . \quad (28)$$

The central value corresponds to the weighted average of the results in Fig. 15 (the average does not include the result from  $b\bar{b}$  mass splitting because of the difficulty in estimating uncertainty in lattice calculations<sup>140</sup>). The errors on the most precise determinations of  $\alpha_S$  are mainly of a theoretical nature and, hence, not Gaussian and highly correlated among themselves. Because of this reason, I have not considered any further reduction of the error

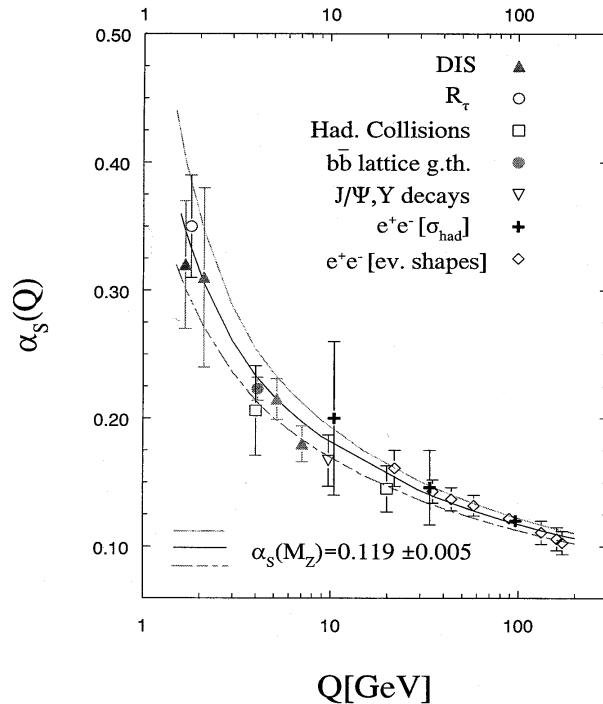


Figure 14: Summary of  $\alpha_s(Q)$ . The lines indicate the QCD predictions in NNLO for three different values of  $\alpha_s(M_Z)$ .

coming from the weighting procedure. The uncertainty quoted in Eq. (28) is equal to the smallest of the errors in Fig. 15.

Different methods, used in recent summaries<sup>141,142</sup> to quote the world average of  $\alpha_S$ , give results similar to that in Eq. (28). Less conservative error estimates ( $\Delta\alpha_S(M_Z) = 0.003$ ) are considered in Refs.<sup>131,132</sup>.

## 7 Concluding remarks

Owing to high-precision experiments and accurate theoretical calculations, perturbative QCD is nowadays very well tested in high-energy hadronic processes. An outstanding example of this is the accuracy on the determination of the strong coupling  $\alpha_S(M_Z)$  and its running. Taken literally, this accuracy implies that in many processes we can control strong-interactions dynamics at short distances to a precision better than 5%. The achieved reliability of perturbative QCD is extremely valuable to estimate SM backgrounds for new-physics signals, although in some cases the insufficient knowledge of the non-perturbative parton densities remains a source of sizeable uncertainty.

Small- $x$  physics deals with a kinematic regime near the borderline between hard and soft collisions and can lead to a QCD understanding of the high-energy behaviour of soft hadronic interactions. In the very near future substantial progress is expected as a consequence of the increasing amount of data and of recent theoretical developments in this field.

The interplay between perturbative and non-perturbative phenomena is one of the main



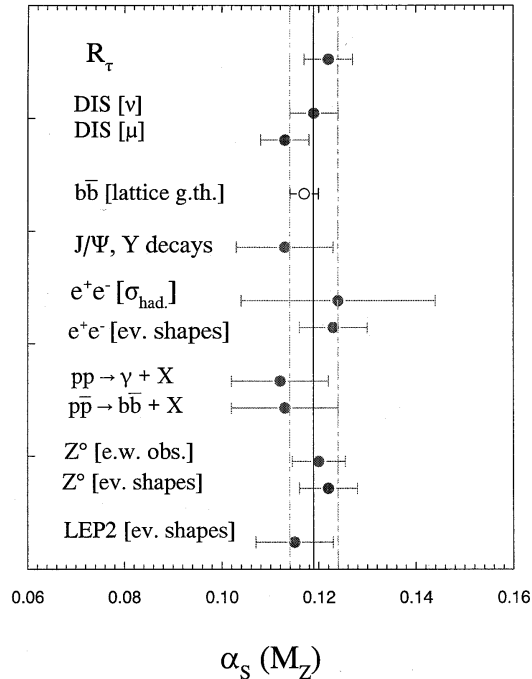


Figure 15: Summary of measurements of  $\alpha_S(M_Z)$ . The band corresponds to the world average  $\alpha_S(M_Z) = 0.119 \pm 0.005$ .

open issues in QCD. In the past few years, methods inspired by perturbation theory have been developed to control non-perturbative power corrections to perturbative predictions. These methods are at present in a stage that is similar to that of LO perturbative calculations at the end of the 70's. Forthcoming phenomenological and theoretical studies along these lines can play an important role in understanding the hadronization mechanism.

## Acknowledgements

I would like to thank Prof. Albrecht Wagner and Dr. Albert De Roeck for their excellent organization of the Symposium and Dr. Thomas Gehrmann for his great help during the Symposium. I am grateful to the many colleagues who provided me with detailed information about recent results. In particular, I wish to thank Siggie Bethke, Phil Burrows, Monica Pepe Altarelli and Heidi Schellman.

## References

1. H. Schellman, these proceedings.
2. V. Chekelyan, these proceedings.
3. A. Brüll, these proceedings.
4. S. Soeldner-Rembold, these proceedings.
5. E. Gallo, these proceedings.

6. O. Schneider, these proceedings.
7. S.G. Gorishny, A.L. Kataev and S.A. Larin, Phys. Lett. 259B (1991) 144; L.R. Surguladze and M.A. Samuel, Phys. Rev. Lett. 66 (1991) 560.
8. K.G. Chetyrkin, Phys. Lett. 391B (1997) 402.
9. T. Hebbeker, M. Martinez, G. Passarino and G. Quast, Phys. Lett. 331B (1994) 165.
10. E. Braaten, S. Narison and A. Pich, Nucl. Phys. B373 (1992) 581; F. Le Diberder and A. Pich, Phys. Lett. 289B (1992) 165.
11. M. Neubert, Nucl. Phys. B463 (1996) 511; M. Girone and M. Neubert, Phys. Rev. Lett. 76 (1996) 3061.
12. S.A. Larin, F.V. Tkachov and J.A.M. Vermaseren, Phys. Rev. Lett. 66 (1991) 862; S.A. Larin and J.A.M. Vermaseren, Phys. Lett. 259B (1991) 345.
13. J. Chyla and A.L. Kataev, Phys. Lett. 297B (1992) 385.
14. J. Ellis and M. Karliner, Phys. Lett. 341B (1995) 397; J. Ellis, E. Gardi, M. Karliner and M.A. Samuel, Phys. Lett. 366B (1996) 268.
15. F.T. Tkachov, Phys. Lett. 100B (1981) 65; K.G. Chetyrkin and F.T. Tkachov, Nucl. Phys. B192 (1981) 159.
16. K.G. Chetyrkin, Acta Phys. Polon. B28 (1997) 725 and references therein.
17. K. Wilson, Phys. Rev. 179 (1969) 1499; K. Symanzik, Commun. Math. Phys. 32 (1971) 49; C. Callan, Phys. Rev. D 5 (1972) 3302; R. Brandt, Fortschr. Phys. 18 (1970) 249; M.A. Shifman, A.I. Vainshtein and V.I. Zakharov, Nucl. Phys. B147 (1979) 385, 448, 519.
18. K. Hagiwara, D. Haidt and S. Matsumoto, preprint KEK-TH-512 (hep-ph/9706331).
19. J. Timmermans, these proceedings; D.R. Ward, Int. Europhysics Conf. on High Energy Physics, EPS 97, Jerusalem, August 1997; *The LEP Electroweak Working Group*, LEPEWWG/97-02.
20. K.G. Chetyrkin, A.H. Hoang, J.H. Kühn, M. Steinhauser and T. Teubner, preprint DESY 97-25 (hep-ph/9711327) and references therein.
21. M. Jamin and A. Pich, preprint IFIC-97-06 (hep-ph/9702276).
22. M.B. Voloshin, Int. J. Mod. Phys. A10 (1995) 2856.
23. CLEO Coll., R. Ammar et al., preprint CLNS-97-1493 (hep-ex/9707018).
24. R.K. Ellis, D.A. Ross and A.E. Terrano, Nucl. Phys. B178 (1981) 421; K. Fabricius, I. Schmitt, G. Kramer and G. Schierholz, Z. Phys. C11 (1981) 315.
25. R.K. Ellis, W.J. Stirling and B.R. Webber, *QCD and Collider Physics* (Cambridge University Press, Cambridge, 1996).
26. W.T. Giele and E.W.N. Glover, Phys. Rev. D 46 (1992) 1980; W.T. Giele, E.W.N. Glover and D.A. Kosower, Nucl. Phys. B403 (1993) 633.
27. Z. Kunszt and D.E. Soper, Phys. Rev. D 46 (1992) 192; S. Frixione, Z. Kunszt and A. Signer, Nucl. Phys. B467 (1996) 399; S. Frixione, preprint ETH-TH-97-14 (hep-ph/9706545).
28. S. Catani and M.H. Seymour, Phys. Lett. 378B (1996) 287, Nucl. Phys. B485 (1997) 291.
29. M.L. Mangano and S.J. Parke, Phys. Rep. 200 (1991) 301 and references therein.
30. Z. Bern, L. Dixon and D.A. Kosower, Annu. Rev. Nucl. Part. Sci. 46 (1996) 109 and

references therein.

31. Z. Bern, L. Dixon and D.A. Kosower, Phys. Rev. Lett. 70 (1993) 2677, Nucl. Phys. B437 (1995) 259; Z. Kunszt, A. Signer and Z. Trócsányi, Phys. Lett. 336B (1994) 529.
32. E.W.N. Glover and D.J. Miller, Phys. Lett. 396B (1997) 257; Z. Bern, L. Dixon, D.A. Kosower and S. Weinzierl, Nucl. Phys. B489 (1997) 3; J.M. Campbell, E.W.N. Glover and D.J. Miller, preprint DTP-97-44 (hep-ph/9706297); Z. Bern, L. Dixon and D.A. Kosower, preprint SLAC-PUB-7529 (hep-ph/9708239).
33. A. Signer and L. Dixon, Phys. Rev. Lett. 78 (1997) 811, Phys. Rev. D 56 (1997) 4031; Z. Nagy and Z. Trocsanyi, Phys. Rev. Lett. 79 (1997) 3604, preprint hep-ph/9708343.
34. G. Rodrigo, Nucl. Phys. Proc. Suppl. 54A (1997) 60; G. Rodrigo, A. Santamaria and M. Bilenkii, Phys. Rev. Lett. 79 (1997) 193; W. Bernreuther, A. Brandenburg and P. Uwer, Phys. Rev. Lett. 79 (1997) 189; P. Nason and C. Oleari, Phys. Lett. 407B (1997) 57, preprint CERN-TH-97-219 (hep-ph/9709360).
35. Z. Trocsanyi, Phys. Rev. Lett. 77 (1996) 2182; W.B. Kilgore and W.T. Giele, Phys. Rev. D 55 (1997) 7183.
36. G.R. Farrar, preprint RU-97-82 (hep-ph/9710395) and references therein.
37. DELPHI Coll., S. Cabrera et al., Delphi 97-74 Conf 70, submitted to this Symposium.
38. See: G. Sterman, in *Proc. 10th Topical Workshop on Proton-Antiproton Collider Physics*, eds. R. Raja and J. Yoh (AIP Press, New York, 1996), p. 608; S. Catani, preprint LPTHE-ORSAY-97-46 (hep-ph/9709503) and references therein.
39. S. Catani, Yu.L. Dokshitzer, M. Olsson, G. Turnock and B.R. Webber, Phys. Lett. 269B (1991) 432.
40. S. Catani, G. Turnock, B.R. Webber and L. Trentadue, Phys. Lett. 263B (1991) 491.
41. S. Catani, G. Turnock and B.R. Webber, Phys. Lett. 272B (1991) 368 and 295B (1992) 269.
42. N. Brown and W.J. Stirling, Z. Phys. C53 (1992) 629; S. Bethke, Z. Kunszt, D.E. Soper and W.J. Stirling, Nucl. Phys. B370 (1992) 310.
43. G. Dissertori and M. Schmelling, Phys. Lett. 361B (1995) 167.
44. S. Catani, G. Turnock, B.R. Webber and L. Trentadue, Nucl. Phys. B407 (1993) 3.
45. Z. Kunszt, P. Nason, G. Marchesini and B.R. Webber, in 'Z Physics at LEP 1', CERN 89-08, vol. 1, p. 373.
46. S. Catani, in *Proc. 18th Johns Hopkins Workshop on Current Problems in Particle Theory: Theory Meets Experiment*, eds. R. Casalbuoni, G. Domokos, S. Kovesi-Domokos and B. Monteleoni (World Scientific, Singapore, 1995), p. 21 and references therein.
47. TPC/Two-Gamma Coll., D.A. Bauer et al., preprint LBL-35812 (1994).
48. TOPAZ Coll., Y. Ohnishi et al., Phys. Lett. 313B (1993) 475.
49. JADE Coll., P.A. Movilla Fernandez et al., preprint PITHA-97-27 (hep-ex/9708034).
50. L3 Coll., M. Acciarri et al., Phys. Lett. 371B (1996) 137, Phys. Lett. 404B (1997) 390; OPAL Coll., G. Alexander et al., Z. Phys. C72 (1996) 191, Z. Phys. C75 (1997) 193, OPAL-PN281 submitted to this Symposium; ALEPH Coll., D. Buskulic et al., Z. Phys. C73 (1997) 409, paper LP-299 submitted to this Symposium; DELPHI Coll., J. Drees et al., Delphi 97-92 Conf 77, submitted to Int. Europhysics Conf. on High

- Energy Physics, EPS 97, Jerusalem, August 1997.
51. CDF Coll., F. Abe et al., Phys. Rev. Lett. 77 (1996) 438.
  52. H1 Coll., C. Adloff et al., Z. Phys. C74 (1997) 191; ZEUS Coll., J. Breitweg et al., Z. Phys. C74 (1997) 207.
  53. CDF Coll., F. Abe et al., Phys. Rev. D 50 (1994) 2966, Phys. Rev. Lett. 74 (1995) 2626, preprint FERMILAB-PUB-97-286-E (hep-ex/9710008); D0 Coll., S. Abachi et al., Phys. Rev. Lett. 74 (1995) 2632, Phys. Rev. Lett. 79 (1997) 1203; P. Giromini, these proceedings.
  54. P. Nason, S. Dawson and R.K. Ellis, Nucl. Phys. B303 (1988) 607; W. Beenakker, H. Kuijf, W.L. van Neerven and J. Smith, Phys. Rev. D 40 (1989) 54.
  55. E. Laenen, J. Smith and W.L. van Neerven, Nucl. Phys. B369 (1992) 543, Phys. Lett. 321B (1994) 254; N. Kidonakis, J. Smith and R. Vogt, Phys. Rev. D 56 (1997) 1553.
  56. E.L. Berger and H. Contopanagos, Phys. Lett. 361B (1995) 115, Phys. Rev. D 54 (1996) 3085.
  57. E.L. Berger and H. Contopanagos, preprint ANL-HEP-PR-97-01 (hep-ph/9706206).
  58. S. Catani, M.L. Mangano, P. Nason and L. Trentadue, Phys. Lett. 378B (1996) 329.
  59. S. Catani, M.L. Mangano, P. Nason and L. Trentadue, Nucl. Phys. B478 (1996) 273.
  60. G. Sterman, Nucl. Phys. B281 (1987) 310; S. Catani and L. Trentadue, Nucl. Phys. B353 (1991) 183, Nucl. Phys. B327 (1989) 323.
  61. N. Kidonakis and G. Sterman, Phys. Lett. 387B (1996) 867, preprint EDINBURGH-97-3 (hep-ph/9705234).
  62. F. Aversa, P. Chiappetta, M. Greco and J.Ph. Guillet, Nucl. Phys. B327 (1989) 105, Phys. Rev. Lett. 65 (1990) 401; S.D. Ellis, Z. Kunszt and D.E. Soper, Phys. Rev. D 40 (1989) 2188, Phys. Rev. Lett. 64 (1990) 2121; W.T. Giele, E.W.N. Glover and D.A. Kosower, Nucl. Phys. B403 (1993) 633.
  63. F. Nang (for the CDF and D0 Collaborations), preprint FERMILAB-CONF-97-192-E, presented at *32nd Rencontres de Moriond: QCD and High-Energy Hadronic Interactions*, Les Arcs, March 1997.
  64. CDF Coll., F. Abe et al., Phys. Rev. Lett. 77 (1996) 5336 (E ibid. 78 (1997) 4307); D0 Coll., B. Abbot et al., paper LP-197 submitted to this Symposium.
  65. M. Glück, E. Reya and A. Vogt, Z. Phys. C53 (1992) 127, Z. Phys. C67 (1995) 433; A. Vogt, Phys. Lett. 354B (1995) 145.
  66. A.D. Martin, R.G. Roberts and W. J. Stirling, Phys. Lett. 387B (1996) 419.
  67. H.L. Lai et al., Phys. Rev. D 55 (1997) 1280.
  68. J. Huston et al., Phys. Rev. Lett. 77 (1996) 444.
  69. G. Altarelli, these proceedings.
  70. B. Straub, these proceedings.
  71. S. Catani, M.L. Mangano and P. Nason, unpublished.
  72. S. Catani, G. Marchesini and B.R. Webber, Nucl. Phys. B349 (1991) 635; H. Contopanagos, E. Laenen and G. Sterman, Nucl. Phys. B484 (1997) 303.
  73. M.A.J. Botje (for the ZEUS Coll.), preprint NIKHEF-97-028 (hep-ph/9707289), presented at *5th Int. Workshop on Deep Inelastic Scattering and QCD* (DIS 97), Chicago, April 1997.

74. S. Kuhlmann, H.L. Lai and W.K. Tung, preprint MSU-HEP-70316 (hep-ph/9704338).
75. See: J. Kwiecinski, *Acta Phys. Polon.* B27 (1996) 3455; H. Abramowicz, in *Proc. 28th Int. Conference on High-energy Physics (ICHEP 96)*, eds. Z. Ajduk and A.K. Wroblewski (World Scientific, Singapore, 1997), p. 53 and references therein.
76. V.N. Gribov and L.N. Lipatov, *Sov. J. Nucl. Phys.* 15 (1972) 438, 675; G. Altarelli and G. Parisi, *Nucl. Phys.* B126 (1977) 298; Yu.L. Dokshitzer, *Sov. Phys. JETP* 46 (1977) 641.
77. L.N. Lipatov, *Sov. J. Nucl. Phys.* 23 (1976) 338; E.A. Kuraev, L.N. Lipatov and V.S. Fadin, *Sov. Phys. JETP* 45 (1977) 199; Ya. Balitskii and L.N. Lipatov, *Sov. J. Nucl. Phys.* 28 (1978) 822.
78. A. De Rújula, S.L. Glashow, H.D. Politzer, S.B. Treiman, F. Wilczek and A. Zee, *Phys. Rev. D* 10 (1974) 1649.
79. H1 Coll., S. Aid et al., *Nucl. Phys.* B470 (1996) 3; ZEUS Coll., M.Derrick et al., *Z. Phys.* C72 (1996) 399.
80. R.D. Ball and S. Forte, *Phys. Lett.* 335B (1994) 77, *Phys. Lett.* 336B (1994) 77, *Nucl. Phys. B (Proc. Suppl.)* 54A (1997) 163.
81. C. Lopez, F. Barreiro and F.J. Yndurain, *Z. Phys.* C72 (1996) 561; K. Adel, F. Barreiro and F. J. Yndurain, *Nucl. Phys.* B495 (19221) 97.
82. R.K. Ellis, Z. Kunszt and E.M. Levin, *Nucl. Phys.* B420 (1994) 517 (*E Nucl. Phys.* B433 (1995) 498).
83. R.K. Ellis, F. Hautmann and B.R. Webber, *Phys. Lett.* 348B (1995) 582; F. Hautmann, in *QCD and High Energy Hadronic Interactions, Proc. 30th Rencontres de Moriond*, ed. J. Tran Thanh Van (Editions Frontières, Gif-sur-Yvette, 1995), p. 133.
84. R.D. Ball and S. Forte, *Phys. Lett.* 351B (1995) 313, *Phys. Lett.* 358B (1995) 365.
85. J.R. Forshaw, R.G. Roberts and R.S. Thorne, *Phys. Lett.* 356B (1995) 79.
86. S. Catani, *Z. Phys.* C70 (1996) 263, *Z. Phys.* C75 (1997) 665.
87. S. Catani, M. Ciafaloni and F. Hautmann, *Phys. Lett.* 242B (1990) 97, *Nucl. Phys.* B366 (1991) 135; J.C. Collins and R.K. Ellis, *Nucl. Phys.* B360 (1991) 3; E.M. Levin, M.G. Ryskin, Yu.M. Shabel'skii and A.G. Shuvaev, *Sov. J. Nucl. Phys.* 53 (1991) 657.
88. S. Catani and F. Hautmann, *Phys. Lett.* 315B (1993) 157, *Nucl. Phys.* B427 (1994) 475.
89. A.J. Askew, J. Kwiecinski, A.D. Martin and P.J. Sutton, *Phys. Rev. D* 47 (1993) 3775, *Phys. Rev. D* 49 (1994) 4402; J. Kwiecinski, A.D. Martin and A.M. Stasto, *Phys. Rev. D* 56 (1997) 3991.
90. S. Forte and R.D. Ball, in *Proc. Int. Workshop on Deep Inelastic Scattering and Related Phenomena, DIS 96*, eds. G. D'Agostini and A. Nigro (World Scientific, Singapore, 1997), p. 172.
91. J. Blümlein, S. Riemersma and A. Vogt, *Nucl. Phys. B (Proc. Suppl.)* 51C (1996) 30.
92. R.S. Thorne, *Phys. Lett.* 392B (1997) 463, preprint hep-ph/9710541.
93. H1 Coll., C. Adloff et al., *Phys. Lett.* 393B (1997) 452.
94. R.S. Thorne, preprint RAL-TR-97-039 (hep-ph/9708302).

95. V.S. Fadin and L.N. Lipatov, Sov. J. Nucl. Phys. 50 (1989) 712, Nucl. Phys. B406 (1993) 259, Nucl. Phys. B477 (1996) 767; V.S. Fadin, R. Fiore and A. Quartarolo, Phys. Rev. D 50 (1994) 5893, Phys. Rev. D 53 (1996) 2729; V.S. Fadin, JETP Lett. 61 (1995) 346; V.S. Fadin, R. Fiore and M.I. Kotskii, Phys. Lett. 387B (1996) 593; V.S. Fadin, M.I. Kotskii and L.N. Lipatov, preprint BUDKERINP-96-92 (hep-ph/9704267).
96. G. Camici and M. Ciafaloni, Phys. Lett. 386B (1996) 341, Nucl. Phys. B496 (1997) 305.
97. V. Del Duca, Phys. Rev. D 54 (1996) 989, Phys. Rev. D 54 (1996) 4474; V. Del Duca and C.R. Schmidt, preprint EDINBURGH-97-26 (hep-ph/9711309).
98. G. Camici and M. Ciafaloni, preprint hep-ph/9707390; M. Ciafaloni, preprint hep-ph/9709390, presented at *Ringberg Workshop on New Trends in HERA Physics*, Ringberg Castle, May 1997.
99. V.S. Fadin, M.I. Kotskii and L.N. Lipatov, preprint BUDKERINP-97-56, submitted to this Symposium.
100. M. Ciafaloni, Phys. Lett. 356B (1995) 74.
101. R.D. Ball and S. Forte, Phys. Lett. 359B (1995) 362.
102. G. Bottazzi, G. Marchesini, G.P. Salam and M. Scorletti, preprint IFUM-552-FT (hep-ph/9702418).
103. B. Andersson, G. Gustafson and J. Samuelsson, Z. Phys. C71 (1996) 613, Nucl. Phys. B467 (1996) 443.
104. M. Ciafaloni, Nucl. Phys. B296 (1988) 49.
105. S. Catani, F. Fiorani and G. Marchesini, Phys. Lett. 234B (1990) 339, Nucl. Phys. B336 (1990) 18.
106. G. Camici and M. Ciafaloni, Phys. Lett. 395B (1997) 118.
107. A.H. Mueller, Phys. Lett. 396B (1997) 251.
108. A.H. Mueller, in *QCD: 20 Years Later*, eds. P.M. Zerwas and H.A. Kastrup (World Scientific, Singapore, 1993), p. 162 and references therein.
109. See: R. Akhoury and V.I. Zakharov, Nucl. Phys. B (Proc. Suppl.) 54A (1997) 217; M. Beneke, preprint CERN-TH-97-134 (hep-ph/9706457) and references therein.
110. P. Ball, M. Beneke and V.M. Braun, Nucl. Phys. B452 (1995) 563 and references therein.
111. G.P. Korchemsky and G. Sterman, Nucl. Phys. B437 (1995) 415; R. Akhoury and V.I. Zakharov, Phys. Lett. 357B (1995) 646, Nucl. Phys. B465 (1996) 295.
112. M. Beneke and V.M. Braun, Nucl. Phys. B454 (1995) 253.
113. P. Nason and M.H. Seymour, Nucl. Phys. B454 (1995) 291.
114. Yu.L. Dokshitzer, G. Marchesini and B.R. Webber, Nucl. Phys. B469 (1996) 93.
115. I.G. Knowles and G.D. Lafferty, J. Phys. G23 (1997) 731 and references therein.
116. B.R. Webber, Phys. Lett. 339B (1994) 148; A.V. Manohar and M.B. Wise, Phys. Lett. 344B (1995) 407.
117. Yu.L. Dokshitzer and B.R. Webber, Phys. Lett. 352B (1995) 451.
118. DELPHI Coll., P. Abreu et al., Z. Phys. C73 (1997) 243.
119. D. Wicke, preprint hep-ph/9708467, presented at *Int. Euroconference on Quantum*

- Chromodynamics*, QCD 97, Montpellier, July 1997.
120. ALEPH Coll., paper LP-258 submitted to this Symposium.
  121. H1 Coll., C. Adloff et al., Phys. Lett. 406B (1997) 256.
  122. E. Mirkes and D. Zeppenfeld, Phys. Lett. 380B (1996) 205, preprint MADPH-97-1002 (hep-ph/9706437).
  123. S. Catani and M.H. Seymour, Nucl. Phys. B485 (1997) 291, in *Proc. Workshop on Future Physics at HERA*, eds. G. Ingelman, A. De Roeck and R. Klanner (DESY, Hamburg, 1996), p. 519.
  124. D. Graudenz, preprint PSI-PR-97-20 (hep-ph/9708362), preprint hep-ph/9710244.
  125. M. Dasgupta and B.R. Webber, preprint CAVENDISH-HEP-96-5 (hep-ph/9704297).
  126. DELPHI Coll., P. Abreu et al., preprint DELPHI 97-69 CONF 55, submitted to this Symposium.
  127. P.J. Rijken and W.L. van Neerven, Phys. Lett. 386B (1996) 422, Nucl. Phys. B487 (1997) 233.
  128. M. Dasgupta and B.R. Webber, Nucl. Phys. B484 (1997) 247; M. Beneke, V.M. Braun and L. Magnea, Nucl. Phys. B497 (1997) 297.
  129. Yu.L. Dokshitzer, A. Lucenti, G. Marchesini and G.P. Salam, preprint IFUM-573-FT (hep-ph/9707532).
  130. Yu.L. Dokshitzer and B.R. Webber, Phys. Lett. 404B (1997) 321.
  131. M. Schmelling, in *Proc. 28th Int. Conference on High-energy Physics (ICHEP 96)*, eds. Z. Ajduk and A.K. Wroblewski (World Scientific, Singapore, 1997), p. 91.
  132. Particle Data Group, Review of Particles Properties, R.M. Barnett et al., Phys. Rev. D 54 (1996) 1.
  133. CCFR Coll., W.G. Seligman et al., preprint NEVIS-REPORT-292 (hep-ex/9701017).
  134. R.G. Roberts, preprint RAL-TR-97-024 (hep-ph/9706269), presented at *5th Int. Workshop on Deep Inelastic Scattering and QCD (DIS 97)*, Chicago, April 1997.
  135. G. Altarelli, R.D. Ball, S. Forte and G. Ridolfi, Nucl. Phys. B496 (1997) 337.
  136. W.T. Giele, E.W.N. Glover and J. Yu, Phys. Rev. D 53 (1996) 120.
  137. A. Pich, preprint FTUV-97-22 (hep-ph/9704453), to appear in *Heavy Flavours II*, eds. A.J. Buras and M. Lindner (World Scientific, Singapore, 1997).
  138. M. Kobel, in *Perturbative QCD and Hadronic Interactions, Proc. 27th Rencontres de Moriond*, ed. J. Tran Thanh Van (Editions Frontières, Gif-sur-Yvette, 1992), p. 145.
  139. M. Gremm and A. Kapustin, Phys. Lett. 407B (1997) 323.
  140. M. Lüscher, these proceedings.
  141. P.N. Burrows, preprint SLAC-PUB-7631 (hep-ex/9709010), presented at *17th Int. Conference on Physics in Collision (PIC 97)*, Bristol, June 1997.
  142. S. Bethke, preprint PITHA-97-37 (hep-ex/9710030), presented at *Int. Euroconference on Quantum Chromodynamics, QCD 97, Montpellier, July 1997*.

Table 1: A summary of measurements of  $\alpha_s$ .

Process	Q [GeV]	$\alpha_s(Q)$	$\alpha_s(M_{Z^0})$	$\Delta\alpha_s(M_{Z^0})$		Order of perturb.
				exp.	theor.	
GLS sr	1.73	$0.32 \pm 0.05$	$0.115 \pm 0.006$	0.005	0.003	NNLO
$R_\tau$	1.78	$0.35 \pm 0.04$	$0.122 \pm 0.005$	0.002	0.005	NNLO
DIS [polar.]	2.11	$0.31^{+0.08}_{-0.06}$	$0.120^{+0.010}_{-0.008}$	$^{+0.004}_{-0.005}$	$^{+0.009}_{-0.006}$	NLO
DIS [HERA $F_2$ ]	4.5	$0.23 \pm 0.04$	$0.120 \pm 0.010$	0.005	0.009	NLO
DIS [ $\nu$ ]	5.0	$0.215 \pm 0.016$	$0.119 \pm 0.005$	0.002	0.004	NLO
DIS [ $\mu$ ]	7.1	$0.180 \pm 0.014$	$0.113 \pm 0.005$	0.003	0.004	NLO
$b\bar{b}$ mass splitting	4.1	$0.223 \pm 0.009$	$0.117 \pm 0.003$	0.000	0.003	LGT
$e^+e^-$ [ $\Upsilon + X$ ]	4.1	$0.228^{+0.045}_{-0.030}$	$0.119^{+0.010}_{-0.008}$	0.002	$^{+0.010}_{-0.008}$	NLO
$J/\Psi, \Upsilon$ [had. decay]	10.0	$0.167 \pm 0.020$	$0.113 \pm 0.010$	0.001	0.010	NLO
$e^+e^-$ [ $\sigma_{had}$ ]	10.5	$0.20 \pm 0.06$	$0.13 \pm 0.03$	0.02	0.02	NNLO
$e^+e^-$ [ev. shapes]	22	$0.161^{+0.016}_{-0.011}$	$0.124^{+0.009}_{-0.006}$	0.005	$^{+0.008}_{-0.003}$	resum.
$e^+e^-$ [ev. shapes]	29	$0.160 \pm 0.012$	$0.131 \pm 0.010$	0.006	0.008	resum.
$e^+e^-$ [ $\sigma_{had}$ ]	34.0	$0.146^{+0.031}_{-0.026}$	$0.124^{+0.021}_{-0.019}$	$^{+0.021}_{-0.019}$	–	NLO
$e^+e^-$ [ev. shapes]	35.0	$0.143^{+0.011}_{-0.007}$	$0.122^{+0.008}_{-0.006}$	0.002	$^{+0.008}_{-0.005}$	resum.
$e^+e^-$ [ev. shapes]	44.0	$0.137^{+0.010}_{-0.007}$	$0.122^{+0.008}_{-0.006}$	0.003	$^{+0.007}_{-0.005}$	resum.
$e^+e^-$ [ev. shapes]	58.0	$0.132 \pm 0.008$	$0.123 \pm 0.007$	0.003	0.007	resum.
$pp, p\bar{p} \rightarrow \gamma + X$	4	$0.206^{+0.042}_{-0.024}$	$0.112^{+0.012}_{-0.008}$	0.006	$^{+0.010}_{-0.005}$	NLO
$p\bar{p} \rightarrow b\bar{b} + X$	20.0	$0.145^{+0.018}_{-0.019}$	$0.113 \pm 0.011$	$^{+0.007}_{-0.006}$	$^{+0.008}_{-0.009}$	NLO
$p\bar{p} \rightarrow \text{jet} + X$	120	$0.116 \pm 0.009$	$0.121 \pm 0.010$	0.008	0.005	NLO
$e^+e^-$ [scal. viol.]	36	$0.147 \pm 0.014$	$0.125 \pm 0.010$	0.006	0.008	NLO
$Z^0$ [e.w. obs.]	91.2	$0.120^{+0.005}_{-0.004}$	$0.120^{+0.005}_{-0.004}$	0.003	$^{+0.004}_{-0.002}$	NNLO
$Z^0$ [ev. shapes]	91.2	$0.122 \pm 0.006$	$0.122 \pm 0.006$	0.001	0.006	resum.
$e^+e^-$ [ev. shapes]	133	$0.111 \pm 0.007$	$0.117 \pm 0.008$	0.004	0.007	resum.
$e^+e^-$ [ev. shapes]	161	$0.106 \pm 0.007$	$0.115 \pm 0.008$	0.004	0.007	resum.
$e^+e^-$ [ev. shapes]	172	$0.103 \pm 0.007$	$0.112 \pm 0.008$	0.004	0.007	resum.
DIS [av. ev. shapes]	7 - 100		$0.118^{+0.007}_{-0.006}$	0.001	$^{+0.007}_{-0.006}$	NLO + p.c.
$e^+e^-$ [av. ev. shapes]	14 - 172		$0.116^{+0.006}_{-0.005}$	0.001	$^{+0.006}_{-0.005}$	NLO + p.c.
$e^+e^-$ [ $\sigma_L$ ]	91.2	$0.110 \pm 0.016$	$0.110 \pm 0.016$	0.013	0.010	NLO + p.c.